THE FLUVIAL SEQUENCE OF A LATEST CHANGHSINGIAN, PRE-PT EXTINCTION RIVER COMPLEX, EASTERN CAPE PROVINCE, SOUTH AFRICA

Tara Chizinski ‘14

A Thesis

Submitted to the Faculty of the Geology Department of Colby College in Fulfillment of the Requirements for Honors in Geology

Waterville, Maine

May, 2014

THE FLUVIAL SEQUENCE OF A LATEST CHANGHSINGIAN, PRE-PT EXTINCTION RIVER COMPLEX, EASTERN CAPE PROVINCE, SOUTH AFRICA

Except where the reference is made to the work of others, the work described in this thesis is my own or was done in collaboration with my advisory committee.

Tara Chizinski '14

Certificate of Approval:

Dr. Robert A. Gastaldo
Whipple-Coddington Professor
Department of Geology

Dr. Walter A. Sullivan
Assistant Professor
Department of Geology

Dr. Robert E. Nelson
Professor
Department of Geology

ABSTRACT

The Permian–Triassic mass extinction, dated between 251.941 ± 0.037 and 251.880 ± 0.0371 Ma, is well documented in the marine record, but details of the event on land are still ambiguous and widely debated within the scientific community. This project focuses on the stratigraphic record leading up to the PT boundary at one of the critical sections in the Karoo Basin of South Africa, Wapadsberg Pass. A transition in river styles is reported to have occurred across the landscape from meandering Permian sandstone-dominated channels to Triassic braided complexes. This transition can be recorded by architectural elements, which reflect sensitive variations in river flow and composition that could be driven by climate change. A road cut along the R61 at New Wapadsberg Pass exposes a vertical cross section through a channel complex, providing an opportunity to evaluate a latest Changhsingian landscape.

Field work undertaken in January 2012 included: construction of a stratigraphic section; standard lithologic description including grain size, color, and primary structures; and acquisition of several photomosaics from which fluvial architecture could be evaluated. Subsequent methods included a refinement of sandstone classification based on optically measured grain size, QFL ratios, and elemental CHN analyses. Panoramic photomosaics were used to determine bounding surfaces of main channels and internal channel geometries which can be correlated to specific depositional environments.

Based on photomosaic analysis, eight imbricated channels occur in a 40 m thick stratigraphic section. Towards the section base, bounding surfaces are overlain by thin (< 2 m) sandstone or sandy coarse siltstone bedforms, with an overlying thick channel-fill sequence of coarse and fine siltstone. However, at this stratigraphic level, the river system shows a higher proportion of suspension load relative to bedload. Bedload deposits change to coarse sandy

siltstone higher in the section where little sandstone is encountered. Here, there is a significantly higher proportion of bedload, relative to suspension load, with finer grained material making up the channel bed and fill sequences. Hence, the very fine-grained nature of these latest Permian channel fills may be confused with thick paleosol sequences if lateral facies relationships are not taken into account.

ACKNOWLEDGEMENTS

I would like to acknowledge the help and support of Dr. Robert Gastaldo as my advisor, and thank him for the opportunity to travel to South Africa to complete fieldwork for this project. I would also like to thank the research team that helped with fieldwork in South Africa. Thanks to my committee members for their time and help with writing this thesis. This project was made possible through funding from the NSF EAR 1123570 grant, the Selover Family Endowment Fund, and the Dean of Faculty Student Grant Fund at Colby College.

TABLE OF CONTENTS

1. INTRODUCTION

1.1 Overview

The Permian-Triassic extinction event (dated between 251.941± 0.037 and 251.880±0.031 Ma; Burgess *et al*., 2014) resulted in rapid global biodiversity loss, with an estimated disappearance of over 75% of marine genera (Payne and Clapham, 2012) and a corresponding loss of terrestrial biodiversity (Smith, 1995; Ward *et al.*, 2005; Smith and Botha, 2005; Viglietti *et al.,* 2013). However, debate continues over whether extinctions in the marine and terrestrial environments were synchronous or asynchronous (Twitchett *et al.,* 2001; De Kock and Kirschvink, 2004; Gastaldo *et al.*, 2014). Ancient ocean basins provide a more continuous sedimentary record and thus, these environments have been examined more widely for studying the Permian-Triassic Boundary (PTB) (Payne and Clapham, 2012). Exposure of the terrestrial PTB is limited; however, the Karoo Basin of South Africa provides one region where it is exposed surficially. Thus, several localities within this basin have become critical for understanding the details of the extinction event in the terrestrial environment.

The continental PTB currently is defined biostratigraphically by the Last Appearance Datum (LAD) of *Dicynodon lacerticeps* (King, 1990; Rubidge, 1995; Smith and Ward, 2001; Ward *et al.*, 2005). Associated with the biostratigraphic boundary is a supposedly unique lithofacies, an "event bed," characterized by interbeded red and green mudstones, that can be correlated across the basin (Smith and Ward, 2001; Ward *et al.,* 2005). However, it recently has been shown that this "distinct" laminite bed occurs at different stratigraphic positions, relative to the LAD *Dicynodon lacerticeps*, at different critical PTB localities (Gastaldo *et al.*, 2009). Additionally, the bed cannot be traced laterally for any continuous distance (Gastaldo *et al.,* 2009). This calls into question some of the presently accepted characteristics related to the terrestrial record of the PT (Permian-Triassic) extinction in the Karoo Basin. Therefore, it is

important to document these boundary sections in high resolution and address other parameters that have been used to understand the terrestrial extinction event.

One parameter used to separate Permian from Triassic rocks is the style of fluvial deposits across the boundary (Smith, 1995; Ward *et al*., 2000; Michaelsen, 2002; Arche and López-Gómez, 2005). The current model proposes a transition in river character from latest Permian, large meandering channels, to earliest Triassic, shallow braided systems. This transition was accompanied by an increase in aridity across the PTB (Smith, 1995; Ward *et al.*, 2000). Pre-extinction rivers were characterized by wide, stable channels carrying mixed sand and silt incised into a landscape dominated by poorly developed, olive-gray paleosols (Smith, 1990; Ward *et al.*, 2000). This is in contrast to the post-extinction landscape, which is considered to consist of expansive sand-dominated braided systems within maroon paleosols (Ward *et al.*, 2000). Due to the relatively low proportion of channel-to-paleosol deposits that are preserved in ancient landscapes, there are few exposures of these systems positioned near the time of the Permian-Triassic extinction in the Karoo Basin.

One of the critical sections reported to contain the PTB also is well suited for analysis of changes in river architecture leading up to the extinction event. New Wapadsberg Pass is located in the Eastern Cape Province (Fig. 1) where a section of >70 vertical meters spread across ~0.5 lateral kilometers is exposed. The upper 40 vertical meters of the section represents fluvial channel deposits and occurs above a fossiliferous bed in which a *Glossopteris*-rich assemblage is preserved in a paleosol sequence (Prevec *et al.*, 2010). This fossiliferous bed is correlated with another leaf-litter horizon at nearby Old Wapadsberg Pass, a section that has been studied extensively and contains the vertebrate-defined PTB (Prevec *et al.*, 2010; Smith and Botha-Brink, 2014). This megaflora is located about 70 m stratigraphically below the presently defined

PTB (Prevec *et al.*, 2010; Gastaldo *et al.*, 2013). Hence, the New Wapadsberg Pass section provides an ideal context for characterizing a river complex immediately prior to the PTB.

1.2 Historical Context and Background

Historically, The Permian-Triassic Boundary, defined by a mass extinction event, has been studied most extensively in latest Paleozoic marine sections, as such sections provide a nearly uninterrupted record that can be correlated with other marine sequences. Additionally, biological and geochemical data are more easily collected in these rocks because they are abundant and a more complete fossil record is preserved (Coney, 2005; Coney *et al.*, 2007). The marine section at Meishan, China, is the Global Stratotype Section and Point (GSSP) for the Permian-Triassic Boundary where the PTB is defined by the first appearance of the conodont *Hindeodus parvus* (Yin *et al.*, 2001; Yin *et al.*, 2007). Detailed studies of the GSSP and correlated localities have led to a greater understanding of the Permian-Triassic extinction event in the marine environment. The terrestrial extinction is comparatively less well understood and more controversial. Methods for correlating between terrestrial localities, the exact stratigraphic placement of the terrestrial boundary, and the environmental conditions surrounding the terrestrial extinction are still widely debated.

Changes in the Terrestrial Environment across the PTB

The change in terrestrial environmental conditions that occurred as a result of the Permian-Triassic extinction is highly debated. Although it has occasionally been proposed that the extinction in the terrestrial realm occurred independent of that in the marine realm (De Kock and Kirschvink, 2004), it more often has been hypothesized that the two events were synchronous (Twitchett *et al.*, 2001; Metcalfe and Isozaki, 2009; Lucas, 2009). Additionally, interpretations of most studies have suggested that the extinction was a global event and large-

scale environmental changes are mirrored across multiple localities (MacLeod *et al.*, 2000; Arche and López-Gómez, 2005; Twitchett, 2007).

Hypotheses for changing environmental and climatic conditions across the PTB have evolved over time and are still a major topic of concern. Some early models indicated a severe global climatic cooling that was responsible for the majority of floral and faunal die-off (Stanley, 1988; Kozur, 1998). However, data to support these interpretations largely come from marine sequences and have been shown to be unreliable (Twitchett, 2007). Evidence of a cooling event has not been documented in terrestrial localities. The more widely accepted extinction model is that a severe global warming event associated with elevated carbon dioxide levels and depleted oxygen levels occurred across the PTB (Berner, 2005; Twitchett, 2007).

In recent years, computer simulations for climate change across the PTB have been used to assess and refine current models (Twitchett, 2007). These simulations employ various forcing mechanisms to model what changes could have occurred under specific conditions. Results then are compared with rock and fossil evidence to assess model credibility (Twitchett, 2007). Recent simulations incorporating both oceanic and atmospheric conditions match closely with the observed rock record (Kiehl and Shields, 2005; Montenegro *et al.*, 2011). Understanding the mechanisms that drove Permian-Triassic environmental change can be greatly increased with model refinement. This knowledge can provide a more global comprehension of conditions, allowing for studies conducted at the local scale to be placed within this context. However, the strength of any type of simulation-based model for paleoclimate depends heavily on the reliability and extent of environmental data taken from the rock record.

One feature often used to assess environmental change near the PTB is fluvial style (Smith, 1995; Ward *et al.*, 2000; Michaelsen, 2002; Arche and López-Gómez, 2005). Smith

(1995) documented a lithofacies change in the Karoo Basin fluvial deposits where large meandering river channels lost stability in the Early Triassic and transitioned to braided systems. The transition occured relatively quickly and was suggested to represent increasingly arid conditions across the boundary and into the Triassic (Smith, 1995). This idea was reiterated by Ward *et al.* (2000), who propose that a loss of vegetation due to the floral die-off at the Permian-Triassic extinction resulted in decreased soil and channel-bank stability that ultimately led to the development of braidplains. A similar scenario was reported from the Bowen Basin, Australia, where a latest Permian fluvial system, representing a low sinuosity meandering system, is overlain by a braided floodplain environment in the earliest Triassic (Michaelsen, 2002). However, a disconformity attributed to tectonism exists below the Triassic sandstones (Michaelsen, 2002). This change in fluvial style is thought to have been driven by a widespread loss of vegetation. However, Arche and López-Gómez (2005) characterize a sequence in Spain where lithofacies reflect the existence of braided systems beginning in the Middle Permian and extending into the Triassic. Ward *et al.* (2000) noted the existence of a few other similar systems reported from European localities. Because a transition from meandering to braided river systems can be observed across multiple basins, it has been purported that a global mechanism controlled changes in fluvial style across the PTB (Ward *et al.,* 2000; Benton and Newall, 2014). However, discrepancies in some European sections indicate that local variations cannot be ignored in favor of a governing global mechanism (Arche and López-Gómez, 2005). Both local and global variables must be considered when characterizing the fluvial deposits, and associated paleoenvironmental change, of a region.

1.3 Historical Context and Background: The Karoo Basin, South Africa

The Karoo Basin is one of the most widely studied terrestrial PTB localities. Studies have ranged from attempts to understand the causes of the Permian-Triassic extinction (*e.g.* De Kock and Kirschvink, 2004), to fossil surveys (Rubidge, 2005), to analyses of fluvial changes across the PTB (*e.g.* Smith, 1995; Ward *et al.,* 2000). The nearly continuous sedimentary record, extensive vertebrate fossil record, and availability of Permian-Triassic outcrops make the Karoo Basin a highly suitable study region. Additionally, the general history and sedimentary patterns of the basin are relatively well understood, providing a context for studies of the extinction event and PTB.

Karoo Basin Overview and History

The Karoo Basin is one of several Paleozoic to Mesozoic closed sedimentary basins that acted as a site of sediment deposition on the Gondwana super-continent (Smith *et al.,* 1993). Continued sedimentary infill from the basin margins allowed for the accumulation of a relatively complete stratigraphic record (Smith *et al.,* 1993). The Karoo Supergroup is part of this record, and it records approximately 100 Ma of nearly continuous continental sedimentation from the Late Carboniferous (280 Ma) through the Early Jurassic (180 Ma) (Smith *et al.,* 1993; Johnson *et al.,* 2006; Rubidge *et al.,* 2012). Early estimates for the Karoo Supergroup indicated a maximum thickness of about 8,000 m, with the sequence thinning to the northeast (Smith *et al.,* 1993). However, recent studies using seismic imaging techniques show a thinner overall sequence ranging from 2,000 to 5,000 m, with little to no thinning along a north-south transect (Lindeque *et al.,* 2011). This seismic study has initiated new ideas about the Karoo Basin's formation and history.

Ideas regarding the tectonic and sedimentological history of the Karoo Basin have evolved over time with increased research and technology. The traditional model considers the

basin to be a retro-arc foreland basin (Rubidge *et al.*, 2000; Johnson *et al.*, 2006) with sedimentation centered in the depressed area behind a fold-thrust belt, the Cape Fold Belt. This mountain belt is thought to be associated with a magmatic arc, formed from northward subduction of oceanic crust during the Late Paleozoic to Early Mesozoic (Johnson *et al.*, 2006), with the location of subduction relatively close to the margin of the paleobasin. Although some researchers still support this model, recent seismic data have been used to suggest an alternate scenario. Lindeque *et al.* (2011) showed no evidence for the presence of a suture zone below the Cape Fold Belt, which would be expected if northward subduction had occurred. Instead, they propose that subduction actually occurred in a southward direction and that the Karoo Basin formed from downwarping behind the margin of the subducting plate (Lindeque *et al.*, 2011). Following basin establishment, sediment from the margins accumulated in the basin, ending in the Jurassic with the breakup of Gondwana (Johnson *et al*., 1996; Smith *et al.*, 1993).

Karoo Basin Stratigraphy

Five main lithostratigraphic groups dominate the modern Karoo Basin's sedimentary record, representing deposition that began in the Late Pennsylvanian and extended into the Early Jurassic. These are the Dwkya, Ecca, Beaufort, Stormberg, and Drakensberg groups. Figures 2 and 3 illustrate the surficial outcrops (Fig. 2) and stratigraphic placement (Fig. 3) of the main lithologic groups and those units pertinent to this study. The Dwkya Group forms the base of the Karoo sequence and lies unconformably on early Paleozoic and Precambrian rocks (Smith *et al.*, 1993). These rocks are primarily glacial diamictites, sandstones, and shales that were deposited as a result of continental glaciation from the Late Carboniferous through the Early Permian (Smith *et al.*, 1993; Johnson *et al.*, 2006; Catuneanu *et al.*, 2005). Radioisotopic dates constrain

the Dwyka Group at 302 ± 3 Ma to 288 ± 3 Ma, using U-Pb sensitive high-resolution ion microprobe (SHRIMP) analysis of zircon grains (Bangert *et al.,* 1999).

The Dwyka Group is overlain by the Permian Ecca Group (Jordaan, 1981; Smith *et al.,* 1993; Rubidge *et al.,* 2013). The Ecca Group is interpreted to represent a postglacial deltaic environment characterized by glacially-derived sediment being deposited in an inland sea (Jordaan, 1981; Smith *et al.,* 1993). A modern analog is thought to be similar to the depositional setting of the present day Black Sea and surrounding area (Visser and Looke, 1978). Precise dating of this group has been difficult due to the diachronous nature of the boundary between the Ecca and overlying Beaufort Group (Rubidge *et al.,* 1999; Fildani *et al.,* 2007). This results from variable filling of the inland sea, because the transition from marine to fully continental sedimentation was not uniform in time across the basin (Fildani *et al.,* 2007).

The contact between the Ecca and Beaufort groups is placed at the paleoshoreline of the Early-Middle Permian inland sea (Rubidge *et al.,* 2000) and is exposed in the Western Cape Province (Kapupu *et al*., 2010). Although it has been proposed that continental sedimentation of the Beaufort Group may have began in the Late Permian (Fildani *et al.,* 2007), Rubidge *et al.* (2000) redefined the Ecca-Beaufort contact at 300-650 m below its previous position, indicating a significantly earlier age for the base of the Beaufort Group in the Southern Karoo. However, the Beaufort-Ecca contact occurs at different stratigraphic positions across the basin; hence, a single date indicating the timing of the contact would be insufficient. The overlying Beaufort records sedimentation in an environment interpreted to be dominated by fluvial floodplains (Smith *et al.,* 1993), and is the lithostratigraphic interval in which the PTB is recognized. The Beaufort Group continues into the Middle Triassic, where it is overlain by the Stormberg Group (Smith *et al.,* 1993).

The Stormberg and Drakensberg groups were deposited from the Mid-Late Triassic through the Early Jurassic. This part of the Karoo sequence is dominated by fluvial-lacustrine deposits, ultimately transitioning to higher proportions of aeolian lithofacies (Smith *et al.,* 1993). Aeolian deposits are characteristic of the Clarens Formation placed in the Stormberg Group - which has a gradational lower contact, representing the transition from a floodplain environment to a more arid aeolian environment (Holzförster 2007). This contact is defined and correlated across localities based on lithology. Volcanic activity resulting in the emplacement of the Karoo Large Igneous Province began in the Late Triassic and continued through the Early Cretaceous, resulting in the emplacement of the Drakensberg Group. This volcanism has been linked to the breakup of Gondwana and was characterized by numerous basalt flows, as well as dolorite intrusions (Smith *et al.,* 1993). Previous interpretations of the Karoo igneous province suggested that cumulative outpourings of basalt occurred over a relatively long time scale (from 184-178 Ma) (Jourdan *et al.,* 2005). However, recent work based on $^{40}Ar/^{39}Ar$ dating proposes emplacement over a shorter duration, with distinct, brief episodes of igneous activity (Jourdan *et al.,* 2007). The Early Jurassic volcanic deposits represent the end of approximately 100 Ma of sediment deposition in the basin.

The Beaufort Group

The Beaufort Group is divided into two subgroups, the Adelaide and Tarkastad, with the Adelaide comprising the lower part of the stratigraphy. The Tarkastad Subgroup contains most of the Balfour Formation, the Katberg Formation, and Burgersdrop Formations (Rubidge *et al.,* 2013). The PTB in placed within the informal Palingkloof Member, which is the uppermost member of the Balfour Formation (Fig. 3). These lithologic units provide a structure for characterizing sedimentological changes throughout the Karoo Basin.

Beaufort Group sedimentation is particularly relevant to understanding the changing environmental conditions around the time of the Permian-Triassic extinction. Alternating sequences of fluvially derived sandstone, siltstone, and mudstone dominate, and these deposits represent mid-channel, levee, or floodplain environments (Smith, 1980; Smith *et al.,* 1993). There is a reported change in the character of these deposits that has been used as an indicator of paleoenvironmental modification over time. Hence, detailed analyses of Beaufort stratigraphy have been conducted across the Karoo Basin.

Sedimentation patterns are reported to vary throughout the Beaufort Group, with changes in alluvial floodplain characteristics. In much of the Adelaide and Lower Tarkastad subgroups, facies interpreted to represent interchannel deposits dominate, and sandstone bodies, characteristic of fluvial channels, are not laterally persistent (Stear, 1983). Where present, sandstone bodies may represent single-channel or multi-storied channel deposits, indicating a reiteration of a particular channel architecture in the same area (Stear, 1983; Smith *et al.,* 1993). These ribbon-sandstone bodies may obtain a thickness of 3-12 meters and often display wings, indicating frequent overbank flooding (Stear, 1983). These conditions, where wide (tens of meters) meandering (high sinuosity) rivers are interpreted to dominate, generally persist until the time of the Permian-Triassic extinction (Viglietti *et al.,* 2013). Following this, there is a proposed transition to braided systems that occurs within 30 m of the PTB in the Lower Triassic rocks (Smith, 1995; Ward *et al*., 2000; Pace *et al*., 2009) hypothesized to be the result of vegetation die-off (Smith, 1995). A climatic change towards drier more seasonal conditions is suggested to accompany the change in river style (Smith 1995; Ward *et al.,* 2000). Braided systems are characteristic of the Lower Triassic Katberg Formation, where sandstones are found as thick arenaceous units, with a high ratio between sandstone and mudstone (Johnson, 1976). These

units tend to be multi-storied, tabular formations, with each story about 5-10 m thick, that extend laterally over several kilometers. This observed transition in river style is thought to be a delayed result of the PT extinction; however, some issues arise when trying to correlate lithologically defined fluvial sections with the vertebrate-defined PTB.

The delineation of vertebrate biozones in the Beaufort Group aids in correlation between lithologic and biologic stratigraphies (Rubidge, 2005), as well as allowing for more direct correlation between the Karoo Basin and other Permian-Triassic fossil-bearing localities. The Beaufort Group is subdivided into 8 assemblage zones based on the dominance of a particular tetrapod genus (Catuneanu *et al.,* 2005). The *Dicynodon* Assemblage Zone (AZ) is used as the basis to identify the latest Permian deposits in the basin, and its disappearance marks the PTB. Once it was thought that the *Lystrosaurus* Assemblage Zone marked the Early Triassic, but it has been shown that a small overlap occurs between these two biozones. *Lystrosaurus* arose in the Late Permian and several species survived into the Triassic (Catuneanu *et al.,* 2005; Viglietti *et al.,* 2013). The presence of *Lystrosaurus* in association with a reported absence of *Dicynodon* in the stratigraphy is used to identify post-extinction times. Recent CA-TIMS age dates obtained from single zircon grains taken throughout the lower part of the Beaufort Group (Rubidge *et al.,* 2013) help to constrain the biostratigraphic zones, making this classification framework easier to apply to other localities.

Placement of the Permian-Triassic Boundary

The placement of the PTB in the Karoo Basin has been complicated because of an incomplete macrofossil record, the sporadic occurrence of carbonate concretions from which geochemical analyses can be conducted, and the virtual absence of volcanic ash beds that make exact dating and correlation with marine extinction data difficult (De Kock and Kirschvink,

2004). Additionally, there is debate about the placement of the PTB relative to the main extinction event. Several methods for the determination of a precise boundary location have been assessed, including lithological, biological, chemical, and paleomagnetic trends that are used to distinguish Permian from Triassic rocks. Prior to the development of an extensive vertebrate record and the application of chemical and magnostratigraphic techniques, the boundary was defined lithostratigraphically as the contact between the Balfour and Katberg formations (King, 1990; Johnson, 1994; Retallack *et al.*, 2003; Coney, 2005).

With increased fossil exploration and the delineation of biostratigraphic zones for vertebrates (Retallack, 1995; Johnson *et al.*, 1996; MacLeod *et al.*, 2000; Rubidge, 2005; Lucas, 2009), biological markers have become a key tool for identifying the Permian-Triassic transition. The initial biostratigraphic placement of the Karoo PTB was at the First Appearance Datum (FAD) of *Lystrosaurus* (Johnson, 1994; SACS, 1980). However, it has since been proposed that the LAD of *Dicynodon* is a better marker for the boundary (Smith 1995; Smith and Ward 2001; Hancox and Rubidge 2001; Rubidge, 2005). It is now commonly accepted that *Lystrosaurus* first appeared in the Late Permian and was one of few reptilian genera to survive into the Triassic (Hancox *et al.*, 2002; Retallack *et al.*, 2003). Recent investigations have resulted in the identification of additional *Lystrosaurus* species, providing a more detailed understanding of the extinction and survival of this genus across the extinction event (Botha and Smith, 2007). Although species-level identifications have the potential to better constrain the biostratigraphically-determined PTB, these also indicate a more complex relationship between species extinctions and originations around the time of the extinction. Although the vertebrate-defined PTB is widely accepted and used, it has been suggested that this boundary marker may not be reliable for correlating the stratigraphic position of the boundary across far reaching

geographic regions (Angielczyk and Kurkin, 2003). Because of this, other proxies to identify the continental PTB have been utilized to supplement the biostratigraphic record.

Palynological methods have been used to investigate Permian-Triassic sequences from both shallow marine and terrestrial environments. A zone with virtually no fossil pollen, only fungal spores, is commonly preserved in shallow marine PT transitional sites (Visscher *et al.*, 1996; Twitchett *et al*., 2001; Steiner *et al.,* 2003; Coney, 2005). This zone is interpreted to be evidence of the die-off of terrestrial plant life followed by an accumulation of organic debris that underwent decay, as evidenced by a "fungal spike" (Visscher *et al.*, 1996). Steiner *et al.* (2003) document this "fungal spike," and associated LAD of pollen of many Late Permian gymnosperms in the Karoo Basin. However, these data originate from a 1-m thick siltstone interval directly underlying the Katberg Formation at Carlton Heights, ~30 m above the vertebrate-defined PTB (Steiner *et al.* 2003). This disparity, between the LAD of *Dicynodon* and the Karoo fungal spike, has not been widely examined or discussed. Diagenetic alteration of pollen in the southern Karoo has made the establishment of a palynological record difficult (De Wit *et al.,* 2002); thus, palynological studies have not been widely used to investigate the extinction in this basin.

The $\delta^{13}C$ isotopic signature in rocks, and a negative excursion of this proxy in the marine record, has been used as a means to identify the PT extinction event in both marine and terrestrial settings. A negative carbon isotope excursion of 4-7 ppm has been recorded in the stratotype section a Meishan, China, and coincides with the extinction event (Erwin, 1994; Korte and Kozur, 2010). However, $\delta^{13}C$ trends from different localities (pelagic marine, shallow marine, and continental deposits) do not always correlate directly (Korte and Kozur, 2010). For example, Korte and Kozur (2010) suggested that the long-term trend shows a definitive negative excursion

at the PTB, while the short term isotopic trend may vary between localities. This indicates that any data set purported to cross the extinction event must contain $\delta^{13}C$ values for a relatively long time interval for a reliable trend to be observed. Because of the relative absence of carbon sources in the Karoo stratigraphy, a long-term isotopic analysis is difficult. To date, studies have reported isotopic trends over short time scales (Thackeray *et al.*, 1990; MacLeod *et al*., 2000; Gastaldo *et al*., 2014), thus biasing the results. Carbon isotope analysis has not been used extensively in the Karoo Basin, but could potentially provide a means of correlating sections in the basin with other sections globally.

Recently, paleomagnetic data have been used as a means to correlate Permian-Triassic localities across the world from both marine and terrestrial sites (De Kock and Kirschvink 2004; Taylor *et al.,* 2009; Glen *et al.,* 2009). Results of remnant paleomagnetic signatures from both marine and terrestrial sections have recorded a change from reversed to normal polarity near the terrestrial PTB, as presently defined by vertebrate biostratigraphy (De Kock and Kirschvink, 2004; Taylor *et al.,* 2009; Glen *et al.,* 2009). A Reverse-Normal polarity shift occurs below the biostratigraphically defined boundary in both marine and terrestrial sections (De Kock and Kirschvink, 2004; Glen *et al.,* 2009). Because of this, some authors have argued (De Kock and Kirschvink, 2004) that the PTB is better defined and correlated magnetostratigraphically and that the marine and terrestrial extinctions were asynchronous. This idea is opposed by other reports (Taylor *et al.,* 2009; Glen *et al.,* 2009) claiming that the marine and terrestrial extinctions occurred at approximately the same time. Additionally, there is still significant debate about the exact placement and dating of the R-N reversal that underlies the PTB, as presently defined (Steiner *et al.,* 1989; Heller *et al.,* 1995; Taylor *et al.,* 2009; Glen *et al.,* 2009). Paleomagnetic data often can be used as a means of correlating PTB localities; however, an absence of

extensive datasets and overprinting of remnant magnetic signatures by Jurassic intrusive activity has limited the use of this method in the Karoo Basin.

The existence of a lithofacies change in the Karoo Basin, not corresponding to any pre-established change in rock units, has been interpreted as distinct for the PTB. It has been proposed that a "lifeless" bed, or "dead zone", correlates with the biostratigraphic boundary, as defined by vertebrate biostratigraphy, providing another marker for the PTB (Smith and Ward, 2001). However, the basin-wide continuity of this bed has been questioned (Gastaldo *et al.*, 2009; Gastaldo and Neveling, 2012) and it has been shown to be an invalid datum. Although potentially unreliable, this event bed is still widely cited in literature and used as a frame of reference for many Karoo PT localities (Smith and Botha-Brink, 2014).

Currently, the vertebrate-defined PTB is considered to be the standard for the Karoo Basin, with paleomagnetic and geochemical data used to supplement the fossil record. The boundary location is recorded at sites where fossil collection has led to proposed identifications of the LAD of *Dicynodon*. Wapadsberg Pass is one of the critical biostratigraphically measured sections on which several Permian-Triassic studies in the Karoo Basin are based (Coney, 2005; Coney *et al.*, 2007; Gastaldo *et al.*, 2009; Prevec *et al.*, 2010).

1.4 Wapadsberg Pass Locality

History

Wapadsberg Pass, located in the Eastern Cape Province (Fig. 1), is one of the Karoo Basin PTB localities that has been an active site of research over the past two decades (Smith and Botha-Brink, 2014). The site consists of two geographically close exposures <1 km apart (Prevec *et al.*, 2010). The section at Old Wapadsberg Pass is in an erosional gully adjacent to the site of the old, now abandoned, Wapadsberg road. The New Wapadsberg Pass locality is along

the current R61 Highway (Prevec *et al.*, 2010), which replaced the older road in the late 20th Century. A large dolorite intrusion outcrops near the top of the New Wapadsberg Pass section, and it altered the area's paleomagnetic signature (Prevec *et al*., 2010). The stratigraphic sections at Old and New Wapadsberg Pass can be correlated based on a distinct *Glossopteris* litter bed preserved at both sites (Prevec *et al.*, 2010; Gastaldo et al., 2014).

Several PTB studies have used the Wapadsberg Pass site, where biostratigraphic and lithostratigraphic studies have been correlated with other localities across the Karoo. The vertebrate-defined PTB has been identified at the Old Wapadsberg Pass site (Ward *et al.* 2000, 2005) based on the vertebrate record here. However, the determination of a unique fossil plant bed at the same stratigraphic datum between Old and New Wapadsberg Pass (Prevec *et al*., 2010), has led to more diversified studies in this area. Megafloral studies include a taphonomic analysis of megaflora assemblages (Gastaldo *et al.*, 2005), systematics of the *in situ* forest-floor litter (Prevec *et al.*, 2010), an evaluation of paleosol trends up to the PTB (Reid *et al.*, 2007), and estimates of paleoatmospheric CO_2 from paleosol carbonate cements (Gastaldo *et al.*, 2014). This site contains many unique elements and has become one of the more widely studied Permian-Triassic sites of the Karoo Basin.

Although Wapadsberg Pass is a well-studied locality, it has not often been used for fully detailing changes in Permian to Triassic river systems. Ward *et al.* (2000) used the section, along with Lootsberg and Old Lootsberg Pass in the immediate vicinity, to document the change in fluvial morphology on either side of the Permian-Triassic boundary. However, Ward *et al.* (2000) presented only a coarse, vertical stratigraphic section. Reid *et al.* (2007) recognized and analyzed aspects of the fluvial architecture preserved at New Wapadsberg Pass, but did not

describe the section in detail. This study examines and characterizes the New Wapadsberg Pass latest Permian river system in high-resolution.

The Present Study

The study section is exposed as a road cut at New Wapadsberg Pass, located along the R61 Highway, Eastern Cape Province, South Africa (Fig. 1). The research focuses on a short stratigraphic section that spans 40 vertical meters, with its base (S 31° 55.968', E 24° 53.142') situated less than 70 m below the PTB as presently defined (Ward *et al.*, 2000, 2005). The top of the section (S 31° 56.047', E 24° 52.952') occurs near a large dolorite intrusion, which is within ~20 m of the biostratigraphically defined boundary. The road cut exposes a transverse to tangential section of a fluvial channel system, approximating a section that appears to be close to perpendicular to paleoflow.

2. MATERIALS AND METHODS

Field work was conducted in January of 2012 using standard field techniques. The section was measured to centimeter-scale resolution using a 1.5-m leveling Jacob's staff and a standard 1-m folding ruler. Vertical measurements totaling 2 or 3 m were taken up the wall of the road cut before a bed was traced horizontally along the road to continue measurements (Fig. 4). This allowed for the creation of a composite vertical stratigraphic section which totals ~42 m. This stratigraphy was supplemented with a series of photographs, compiled into a single photomosaic, that show bounding surfaces separating channels and distinct lateral changes in many beds. As the section was measured, detailed field notes were taken using standard methodologies. Recorded features included: lithology and grain size, Munsell color, primary structures, the presence/absence of concretions, and reaction to hydrochloric acid indicating the presence of carbonate cement. Nineteen hand samples, primarily sandstone and sandy coarse siltstone, were taken through the section and returned to the laboratory for further analysis. To augment the coarse-grained lithologies, a few samples of siltstone also were taken.

Thin sections of all samples were prepared by Applied Petrographic Services, Inc., in Greensburg, Pennsylvania. The grain size for field-identified sandstone samples was examined in thin section using a 300-point-count technique on a petrographic microscope. Grains were selected across a randomized series of transects using a Nikon Eclipse LV100POL microscope, with photomicrographs obtained using a Nikon DS-Ri1 camera mounted on the microscope. Three hundred grains were measured at the micrometer scale, allowing samples to be classified definitively as either a sandstone or siltstone lithology. Samples that contained >50% sand-sized clasts were classified as a sandstone. Those with a greater proportion of silt-sized clasts were classified as a coarse siltstone. Ultimately, 5 sandstone samples, originating from the

middle and upper parts of the section, were assessed further. For these samples, additional sand grains were measured to bring the total number of sand-sized clasts to 300. Folk statistics were used to analyze size distribution of the sand grains. A mineralogical analysis was conducted on these 5 sandstones to determine the proportion of quartz, feldspar, and lithic fragments (also using a 300 point-count technique) with a Leica DM750P petrographic microscope. Fourteen siltstone samples were analyzed for Total organic carbon (TOC) and nitrogen (TON) content using a Perkin Elmer 2400 Elemental Analyzer to possibly determine the contribution of organic matter to these sediments.

Photographs were compiled into a single photomosaic using Adobe Photoshop. The photomosaic was printed on a plotter at a large scale and overlaid with acetate, allowing for all visible bounding surfaces to be traced. Different lithofacies were delimited for the section based on field descriptions of lithology, grain-size, mineralogy, primary structures, and overall geometric features. Each lithofacies was color-coded, on the overlay to identify facies transitions within and across bounding surfaces. This highlighted changes in sedimentation patterns horizontally and vertically in the section. A series of photographs of the colored overlay were compiled into a second photomosaic that was used to create a digitalized version of the facies diagram. Bounding surfaces identified on the photomosaic were classified based on Miall's (1996) classification scheme and used to interpret architectural elements.

Bounding surfaces of 1st through 5th order are found in the Wapadsberg Pass section. 1st order surfaces represent bounding surfaces within beds, separating cross bed sets. 2nd order surfaces are coset bounding surfaces that indicate changes in flow conditions, but not a time lapse. 3rd order surfaces are cross-cutting erosional surfaces within macroforms. 4th order surfaces constitute the upper contact of macroforms. 5th order surfaces are erosional boundaries

that constrain whole channel fill complexes. These 5^{th} order surfaces are used in the Wapadsberg Pass section to delineate individual channels.

3. RESULTS

The section at New Wapadsberg Pass consists of alternating siltstone and sandstone sequences, with no lithologies coarser than fine sandstone. Beds have a depositional dip of approximately 4° to the NE with a strike of about 279°. The section has a total thickness of 40 m. The section consists of 8 zones of relatively coarse (sandy coarse siltstone-sandstone) lithologies separated by finer siltstones. The coarser lithologies are generally a light greenish/yellowish gray, whereas the siltstones tend to be a darker, olive green/gray color. This color difference makes it possible to recognize lithologic changes on a photomosaic of the section (Fig. 5).

In general, coarser lithologies dominate towards the top of the section, and finer lithologies dominate towards the bottom. As such, the thickness of siltstone sequences in between coarser units decreases up section. Figure 6A shows the composite stratigraphy for the entire section, along with descriptions and stratigraphic locations of samples that were used in qualitative grain-size analyses. This figure also indicates the presence of primary and secondary structures within beds.

Primary and secondary sedimentary structures are most easily recognized in the lower half (0-20 m) where the rocks are least affected by a dolorite intrusion located near the top of the pass. Primary structures include laminations, ripples, cross beds, and mud chips. Secondary structures in the form of non-carbonate-cemented nodules are also present, both scattered throughout beds and in distinct horizons. In some cases, bed sequences are recognizably organized into large-scale crossbeds in the lower half of the section.

3.1 High-Resolution Stratigraphy

The Wapadsberg Pass stratigraphic section is primarily composed of 8 architectures. These are delineated based on erosive 5^{th} order bounding surfaces. Each architectural unit is

bounded above and below by a 5th order surface. These units are label by numbers 1 through 8, with 1 being the stratigraphically lowest and progressing up through the stratigraphy. Underlying unit 1 is a section that may have an erosive lower contact, but this would be below the study section and cannot be verified.

The section starts with a carbonate-cemented siltstone sequence, which persists up to 2.25 m (Fig. 6A). Above this, all lithologies contain a non-carbonate matrix. A predominance of fine siltstone, with some coarse siltstone beds, exists from 2.25 m to about 10 m, with some beds containing nodules, isolated medium quartz-sand grains, or cross-beds. Three thin (<5 cm) claystone beds, representing volcanic ash deposits, are also found within this interval.

Unit 1 begins at about 10 m, where a 0.75-m-thick sandstone body lies on top of a 5th order erosional base that separates it from the siltstones below. On top of this sandstone body is a package of fining upward sequences, from sandy coarse siltstone to fine siltstone. Unit 2 contains a basal coarse-grained bed which is approximately 0.75 m thick and grades from very fine sandstone to coarse siltstone. Overlying this, the section between 13-17 m contains a sequence of predominantly fine siltstone with nodules. Unit 3 first appears at 17 m, and has a maximum thickness of ~1.5 m. This unit contains a very fine sandstone that is overlain by a 1-m-thick fine siltstone sequence ending at 19.5 m.

This pattern of coarser-grained units overlying an erosive base and consisting of finer-grained units above continues throughout the section. Units 4, 5, 6, and 7, and 8 begin at 19.5 m, 24 m, 30 m, 34.5 m, and 37.5 m, respectively (Fig. 6A). Unit 4 has a basal coarse-grained layer of about 1 m; however, all other coarse-grained components (Units 5-8) have a thickness of >2 m. The fine-coarse siltstone components that overlay sandstone/sandy coarse siltstone beds vary

between 0.5 and 4 m thick, with these thicker sequences towards the bottom of the section (Fig. 6A).

The designation of architectural units within the stratigraphy provides a basis for interpretations of the extent and character of paleochannels. The 5^{th} order bounding surfaces marked on Figure 6A show the erosional contacts at the base of each new channel. The identification of lithofacies also aids in channel distinctions by providing a division of channel-fill complexes into bedload and suspension-load deposits.

3.2 Lithofacies

A high-resolution stratigraphic analysis of the New Wapadsberg Pass Section has allowed for a total of 10 distinct lithofacies to be identified. These lithofacies include: (1) a very fine/fine wacke sandstone, (2) a sandy coarse siltstone, (3) a coarse siltstone, (4) a coarse siltstone with nodules, (5) an alternating fine-and-coarse siltstone, (6) a carbonate-cemented siltstone, (7) a fine siltstone, (8) a fine siltstone with nodules, (9) a fine siltstone with dispersed quartz grains, and (10) a claystone. Defining characteristics of these lithofacies are summarized in Table 1. Lithofacies are categorized primarily based on grain-size, as well as distinctive features such as the presence/absence of nodules and carbonate in the rock. Figure 6B shows a diagram of lithofacies changes throughout the section. Lithofacies 3 through 10 dominate in the lower half of the section, whereas lithofacies 1 and 2 are more prominent towards the top of the section.

Very Fine/Fine Wacke Sandstone - This facies is characterized by a lithology that is nearly an even mix of sand and silt grains, but with > 50% sand as determined through a point-count analysis. These units are quartz or lithic wackes that are moderate-poorly sorted, negatively skewed, and mainly platykurtic. The sandstone is organized into beds that are either

planar or lenticular in geometry and may show evidence of lateral accretion (Fig. 7A). Beds range from 0.5-3 m thick. Some beds exhibit millimeter-scale ripples at the top. These units are generally underlain by 5^{th} order bounding surfaces and upper contacts may be sharp or gradational. Color ranges from greenish gray (5GY 6/1) to yellowish grey (5Y 6/1-8/1, 5Y 6/2-7/2) to very light grey (N8). Due to the erosional lower contacts, coarse grain size, and ripples these units are interpreted to represent bedload deposits and are used as the basis for delineation of individual channels.

Sandy Coarse Siltstone - This facies is characterized by a lithology that is nearly an even mix of sand and coarse silt, but with > 50% silt, as determined through a point-count analysis. These beds are typically planar, but occasionally lenticular, with a thickness of up to 2 m. Some planar beds of < 0.3 m are encountered towards the bottom of the section (Fig. 7B). Some beds exhibit millimeter-scale laminations or ripples, whereas others are weathered and rubbly. Several beds are thick (~2 m) units in the upper 15 m of the section and show evidence of lateral accretion. Contacts may be erosional, sharp, or gradational below, and sharp or gradational above. Color ranges from greenish gray to light yellowish gray (5GY 5/1-6/1, 5Y 5/1-8/1, 5Y 6/3, 5Y 6/2-7/2). Sandy coarse siltstone units with erosional lower contacts represent bedload deposits.

Coarse Siltstone - This facies is characterized by a dominance of coarse silt sized grains. Many beds contain minimal fine sand grains (< 10%) incorporated into the siltstone matrix. Beds are 0.1-0.9 m in thickness. Beds can be planar or lenticular. Upper and lower contacts may be either sharp or gradational. Color ranges from olive grey (3/1-6/1) to greenish gray (5GY 5/1-6/1).

Coarse Siltstone with Nodules Facies- Coarse siltstone facies as described above, with small (2-5 cm), non-carbonate cemented nodules that occur in distinct horizons. Beds are planar, and between 0.3 and 0.7 m thick. Upper and lower contacts are sharp.

Alternating Fine/Coarse Siltstone - This facies is characterized by fining upward sequences of coarse to fine siltstone that are in beds less than 0.3 m in thickness. The basal coarse siltstone is generally thicker than the overlaying fine siltstones (Fig. 8A), and units are planar, but may have lenticular fine siltstone components at the top. In some cases, these alternating coarse/fine siltstone sequences are organized into large-scale (>1 m thick, >2 m lateral extent) crossbeds. Contacts are sharp below, and may be sharp or gradational above. Color is light olive gray (5Y 5/2) to yellowish (5Y7/2) to greenish gray (5GY 5/1).

Carbonate Cemented Siltstone - This facies consists of coarse and fine siltstone cemented with a carbonate component that strongly effervesces. Fine sand or coarse silt grains (<10%) are incorporated with finer sediment in several beds. Planar beds range from ~0.1-0.3 m in thickness, with a few isolated lenticular beds of no more than 0.2 m at the crest. Color ranges from light olive gray (5Y 4/1-6/1) to greenish gray (5Y 5/2-6/2).This lithofacies is only found in a short interval in the stratigraphic section, beginning at 0 m and extending up to 2.25 m (Fig. 6B).

Fine Siltstone - Fine siltstones are uniformly composed of fine silt-sized grains. Beds generally are greater than 0.1 m in thickness, averaging 0.15-0.2 m and exhibit planar geometries. Several beds show gradational upper and lower contacts with coarse siltstone. Primary structures include millimeter-scale laminations and ripples on some beds, and millimeter-scale mudchips also are present in isolated occurrences. Color ranges from light olive gray to dark greenish gray (5Y 5/2-7/2, 5Y 3/1-6/1, 5GY 3/1-6/1).

Fine Siltstone with Nodules - This facies is similar to the Fine Siltstone described above with the addition of small (2-5 cm), non-carbonate cemented nodules occurring in at least 5 distinct, horizontally-oriented, horizons. This facies is found at one stratigraphic level, beginning at 14.5 m and extending to 16.5 m. The unit has a sharp upper and lower contact. The color is dark greenish grey (5GY 3/1).

Fine Siltstone with Dispersed Quartz Grains- Fine siltstone facies as described previously, with light-colored, fine-sand-sized grains evenly dispersed throughout the lithology. Grains were initially thought to be feldspar in composition when viewed in the field, but were later identified as quartz during thin section analysis. This facies has a planar geometry and attains a thickness of 0.75 m. It can be found throughout the lower 25 m of the section. Contacts with overlying units may be sharp or gradational. Color ranges from olive (5Y 4/1) to light olive (5Y 6/1) grey.

Claystone- This facies consists of claystone in thin (<0.05 m), isolated beds, all of which are located in the lower third (0-13 m) of the section (Fig. 8B). The beds may be rippled or planar, with sharp upper and lower contacts. Claystones are weathered to a color of light greenish gray (5GY 8/1) or yellowish gray (5Y 8/1).

3.3 Total Organic Carbon: Total Organic Nitrogen

Selected siltstone beds were assessed for total organic carbon and nitrogen content. TOC ranges from a minimum value of 0.26 at a stratigraphic position of 7 m to a maximum of 0.75 at 4.55 m (Table 2). TON ranges from a low of 0.04 (31.69 and 36.50 m) to 0.10 (30.21 m; Table 1). TOC:TON ranges from 4.59 at a stratigraphic position of 7 m to 14.13 at 4.55 m (Table 2), with all values less than 15.0. The average TOC:TON value for the samples was 8.49. Figure 6C shows trends in the TOC:TON ratio throughout the section.

3.4 Sandstone Petrography

Sandstones are fine to very fine wackes with the sand-sized grains only slightly dominating thin sections over finer clasts. Of the 8 samples identified as sandstone in the field, only 5 were found to have a >50% proportion of sand-sized clasts (Table 3). The other 3 samples are sandy coarse siltstone based on the ratio of sand to silt and grain size data.

3.4.1 Grain Size Analysis

Grain-size distribution statistics of the five sandstone samples (17.01.01, 17.01.02, 18.01.05, 18.01.16, 18.01.17) are based on Folk statistics (Folk and Ward 1957). Figure 7 shows grain-size distribution histograms for the sandstone samples. The mean grain size of the sample suite ranges from 2.27 Φ (18.01.17 @ 25.50 m) to 3.01 Φ (18.01.05 @ 34.46 m). Therefore, these samples are classified as fine to very fine sandstones. Similarly, the median grain size ranges from 2.16 Φ (18.01.17 @ 25.50 m) to 3.09 Φ (18.01.05 @ 34.46 m), also indicating a composition of fine to very fine sand. Standard deviation values between 0.70 and 1.03 indicate that these samples are moderately to poorly sorted. Skewness ranges from -0.23 to 0.06 (coarse skewed-nearly symmetrical). Kurtosis indicates a distribution that is platykurtic to mesokurtic with values from 0.72 to 1.05. Measured values for the 5 sandstone samples are given in Table 4.

3.4.2 Mineralogy

The wacke sandstone samples are generally quartz and lithic-dominated, with a minor feldspar component (Fig. 9; Table 5). QFL ratios range from 89:2:9 (@ 10.39 m; Sample 17.01.01) to 53:7:40 (@ 25.50 m; Sample 18.01.17). Mineralogical components in sample 18.01.05 (@ 34.46 m) could not be accurately identified because the sample was altered by the dolorite intrusion near the top of the section.

Some characteristics of quartz and lithic grains were noted in thin section. Quartz grains are generally not elongated and are monocrystalline. Some of these grains display undulose extinction. No distinctive characteristics were observed with lithic grains. Feldspar grains are classified as orthoclase, due to the absence of polysynthetic twinning. These characteristics provide insight into source rock materials for the grains.

3.5 Analysis of Bar Complexes

Three bar complexes of at least 2 m in thickness are identified at the base of channel forms exposed in the upper half of the section at stratigraphic positions of 24, 30, and 34.5 m (Fig. 10). These are identified on the basis of the presence of a thick, coarser-grained basal unit, some of which show evidence of lateral accretion. Evidence for lateral accretion includes 3rd or 4th order bounding surfaces within a basal unit that are inclined to 5th order surfaces (Fig. 11; Section A). These are composed primarily of wacke sandstone or very sandy coarse siltstone (Fig. 10). Sand bar 1 (Fig. 10) consists of a coarsening upward sequence in which the grain size changes from sandy coarse siltstone, to sandier coarse siltstone, to a nearly even sand-silt mix (170:167), culminating in a very fine silty sandstone at the top of the structure. The unit has a thickness of 2 meters, and the coarsening sequence occurs over approximately two-thirds of the feature. The bar complex continues for almost 1 m above the uppermost sample for this unit, which is characterized as a very fine lithic wacke. Of the two true sandstone samples from this complex (17.01.02: about halfway up the barform, and 18.01.17: about two-thirds of the way up the barform), the lower sample (17.01.02) at a stratigraphic height of 25 m is more coarsely skewed (finer grains comparatively more abundant) and has a higher ratio of quartz-to-lithic grains (Fig. 10; Table 5). The upper sample from a stratigraphic height of 25.5 m has a more

symmetrical grain-size distribution and a lower quartz-to-lithic ratio, with a higher feldspar component (Fig. 10; Table 5).

Although mineralogical trends within barforms 2 and 3 (Fig. 10) are not identified, these units show similar patterns in grain size changes throughout the unit. The second barform (@ 30.00 m) is characterized as a sandy coarse siltstone that is coarser at the base (Fig. 10). The unit is underlain by a coarse siltstone bed of the same color. The top of the barform consists of a fining upward bed of a slightly more yellowish color. Barform 3 (@ 34.5 m) consists of basal sandy coarse siltstone that grades upwards to fine sandstone and then to the top is a sandy coarse siltstone. Although both barforms show a similar trend in grain size, but barform 2 has an overall finer average grain size (Fig. 10).

3.6 Photomosaic Analysis

Evaluation of a photomosaic of the section allows for the identification of lateral, as well as vertical, lithofacies relationships on a larger scale that may not be noticed based on litholostratigraphic analysis, alone. Figure 5 shows the complete photomosaic and Figure 11 shows digital tracings of several sections which have been color-coded based on lithofacies. Higher order bounding surfaces are also shown on the diagrams. The section contains at 8 units underlain by 5^{th} order bounding surfaces. Each channel sequence is stacked above and to the SE of the previous unit. In the lower part of the section (Fig. 11, Section B) sandstone beds are laterally offset and separated by SE-dipping 3^{rd} order bounding surfaces. This indicates SE-directed lateral accretion. In the lower part of the section, cross bedding is evident in the thicker siltstone sequences (Fig. 11, Sections A and B). Lenticular and discontinuous features are more prominent in the lower part of the section, with beds become, in general, more planar and laterally persistent up section.

Photomosaic analysis also allowed for an estimate of the width and depth of the observed channel units. Channel width is likely at least 40 m, as at least 20 m lateral extent is seen for each channel, which is assumed to be approximately half of the overall channel width. Channel depth is no more than 6 m, as this is the thickest channel-fill sequence measured. These estimates provide and understanding of the overall geometry of the channels.

4. DISCUSSION

The Wapadsberg Pass fluvial channel system provides insight into latest Permian river systems and their relationship to climate change just prior to the PTB. This stratigraphic section contains 8 channel bases and their associated channel fills, with a thick channel-fill sequence underlying the first channel base. These channels range in thickness from 2-6 m. They are underlain by 5th order erosive surfaces.

The sequence of channel fills documented in this section shows a distinct change in the proportions of bedload to suspended load deposition. There is a higher proportion of fine-grained suspension-load channel-fill in the lower part of the section whereas a transition to a bedload-dominated system occurs beginning at ~30 m stratigraphic height. This transition in depositional style is best displayed in the upper 10 m of the section.

The Wapadsberg Pass system of rivers is interpreted to represent a series of low-energy meandering channels that migrated across the landscape. As this migration occured, floodplain aggradation allowed for the distinct pattern seen in this section, where subsequent channels are both stacked on and offset from the previous iteration. The system shows evidence of a change in flow/sediment load conditions up section; however, there is no evidence for a definitive change in river morphology.

4.1. Lithofacies Interpretations

Claystone Lithofacies

This light gray lithofacies is interpreted as the product of volcanic ash that was transported downstream and deposited in the river system. The sharp contrast in color between claystone beds and the surrounding siltstones indicate a different source, and detrital zircon

grains have been obtained from one of these beds. These can provide a maximum age for that bed of 252.0 ± 0.5 Ma (unpublished results).

Siltstone Lithofacies

The group of siltstone lithofacies includes coarse siltstone; coarse siltstone with nodules; alternating fine and coarse siltstone; carbonate-cemented siltstone; fine siltstone; fine siltstone with nodules; and fine siltstone with dispersed quartz grains. These lithofacies are interpreted to represent the channel-fill sequences where sediment settled out of suspension following channel abandonment. Differences in grain size are a reflection of the energy of the river at the time of deposition, with larger grains requiring a higher energy for transport than smaller grains. Contacts between beds and facies often are gradational, as the river's energy will change slightly over time. Additionally, variability in river currents, water speed, and turbidity across the channel can cause a lateral difference in grain size (Allan and Castillo, 2007).

An anomaly exists with the medium sand-sized quartz grains seen in a few siltstone beds in the lower third of the section (~3 m, ~4.5 m, and ~12.5 m). This difference in grain size in the same bed is not typical for low-energy meandering river sequences (Miall, 1996). These grains may be evidence of a few brief higher-flow events that deposited coarser material within a channel-fill sequence. This supports the idea of flow variability through the channel system during the fill sequence for this meandering river system.

Sandy Coarse Siltstone and Sandstone Lithofacies

These lithofacies are interpreted to represent the bedload deposits and bar forms in the Wapadsberg Pass channels. Although sandy coarse siltstone makes up part of the channel fill in thin beds in the lower half of the section (Fig. 9), this facies most often represents bedload deposits, and is compositionally similar to the silty sandstones found in this section. These units

are interpreted as bedload due to the presence of ripples, evidence of lateral accretion in some macroforms, and the fact that these represent the coarsest deposits in the sequence. These bedload sediments were carried along the base of the channel and deposited as either the result of slowing water or the dominance of friction forces over the forward energy of the water.

4.2. Interpretation of Stratigraphy

The 40 m of vertical composite stratigraphy measured at Wapadsberg Pass is divided into a lower, middle, and upper section, with the lower section containing 2 subdivisions (sections A and B) (Fig. 12). Stratigraphic heights for section boundaries and channel bases, and the thickness of units, are indicated on the composite stratigraphic column (Fig. 6A). The lower section ranges from 0 m to approximately 24 m, with section A (lowermost) comprising 0-17 m and section B comprising 17-23.5 m. Each subdivision of the lower section contains 2 channel-fill sequences. The middle section spans approximately 23.5 m to 30 m, and contains one channel. The upper section ranges from 30-40 m, consisting of the final three channel-fill sequences (Fig. 12).

Lower Section (0-23.5 m)

Section A

Section A comprises the first 17 m of the measured section. This includes just over 10 m of predominantly fine-and-coarse siltstone deposits before the first erosional contact of a channel base is identified (@ 10.39 m). Channel units 1 and 2 are also included in section A. This subsection is characterized by bedload deposits of approximately 0.5 m, relative to suspension-load deposits of 1-3 m.

The Wapadsberg Pass section begins in a zone of carbonate-cemented fine and coarse siltstones. This basal sequence may be a channel-fill interval, but this cannot be confirmed as the

identifying erosive base would fall below the study section in a covered area. This represents a sequence that has been diagenetically altered to include a carbonate cement. Immediately above the carbonate-cemented siltstone interval is a continuation of the initial sequence, although subsequent rocks do not contain carbonate. This indicates a chemical change that no longer allowed for the precipitation of carbonate minerals. Carbonates are not seen in any other rocks throughout the section. This transition represents an environmental change in the lowermost part of the section. The formation of early diagenetic calcite reflects high rates of methanogenesis (Talbot and Kelts, 1986), indicating an anoxic environment.

The base of the first channel that can be positively identified on the photomosaic occurs at ~10.5 m on the composite stratigraphic column (Fig. 11; Fig. 6A). Its position is marked by the first appearance of an increase in sand grains, the presence of ripples, and an erosive basal contact. A sand bar is interpreted to lie above the base of this paleochannel (Fig. 11, Section A) based on its limited lateral extent (5 m), lenticular geometry, and a thickness of 0.5 m at the crest of the structure. A 1.5 m interval of coarse and fine siltstone channel-fill overlies the lenticular barform and cross bedding is visible in some areas. The crossbeds follow the dip of the erosive channel base near the barform (Fig. 11). At the SE end of this channel exposure, siltstone beds dip slightly to the NW, indicating the presence of a base or a low point in the paleochannel.

The channel-fill sequence of channel 1 is eroded into by a stratigraphically higher second channel (Figs. 11, 12). This 2nd channel basal deposit grades from fine sandstone to sandy coarse siltstone within 0.5 m (based on composite stratigraphy), and ~2.5 m of fine-grained channel-fill lies above the basal sandstone. This exposure indicates that a significant amount of suspended-load versus bedload deposition characterizes this sequence. There are at least 5 distinct

horizontal nodule horizons in this channel-fill interval, suggesting bedding planes allowed for later mineral precipitation (Viglietti *et al.*, 2013).

Section B (Channels 3 and 4: ~1 m Bedload, 1-3 m Suspended Load)

Section B comprises the area between 17 and 24 m in the vertical stratigraphy. This section includes channel units 3 and 4. These channel systems lie stratigraphically above channels 1 and 2 from section A. These channels contain a high suspension to bedload ratio, similar to channels 1 and 2. Basal surfaces of these channels are incised into the previously deposited channel-fill sequences (Figs. 11, 12) and each is characterized by a bedload sequence of ~1 m in thickness, followed by fine- to coarse siltstone suspension-load deposits. There is ~1 m (3^{rd} channel) to 3 m (4^{th} channel) of channel fill. Section B is primarily characterized by a relatively high ratio of suspended load to bedload deposits, although bedload units are about twice as thick as those of Section A.

Middle Section

The middle section ranges from 24-30 m and consists of channel unit 5. The middle section is separated from the underlying and overlying channel deposits due to the fact that it contains both thick bedload and suspended load sequences. An erosional surface at ~24 m in the stratigraphy marks the 5^{th} channel-fill sequence and the base of the middle section. The character of this channel is slightly different from those below in that there is a thick (>2 m) sandy coarse siltstone to very fine sandstone bedform above the basal channel bounding surface. This is overlain by a 3-4-m-thick channel-fill sequence that consists of coarser siltstone, differing from the channel-fill sequences lower in the stratigraphy. This channel is interpreted to represent a transition in the sedimentological regime from channels with relatively thin bedload deposits

overlain by thick suspension-load deposits to those with a higher proportion of bedload deposition.

Upper Section

The upper section ranges from 30 m to the top of the study area at 40 m. This includes the uppermost 3 channel deposits (channel units 6, 7, and 8), which consist of >2 m sequences of basal sediments that vary from sandy coarse siltstone to sandstone and are overlain by minimal fine-grained channel-fill. This relationship indicates a predominance of bedload sediment with limited deposition of sediments derived from suspension load deposition. This river character differs significantly from the character of channels lower in the stratigraphy.

4.3. Implications of TOC:TON Measurements

The ratio of TOC to TON in lithified sediment can be used as an indicator of the principal contributor of organic material into a system (Meyers, 1994; Kaushal and Binford, 1999). C:N ratios are minimally altered by diagenesis, allowing them to be useful indicators of organic matter contributions in the distant past (Meyers, 1994). Algal biomass has a C:N ratio that ranges between 4 and 10, while most terrestrial plants have a C:N ratio >20 (Meyers, 1994). This difference is due to the abundance of cellulose in vascular plants, relative to its absence in algae (Meyers, 1994). This signal provides insight into the source of organic material. TOC:TON values in the Wapadsberg Pass siltstones range from a minimum of 4 to a maximum of 14. Values >10 are found in the lower and middle stratigraphies and are interpreted to indicate contribution from a mixed organic source; both algal and terrestrial plants were responsible for OM input. Consistent values ranging from 6 to 8 occur in the upper part of the section and are indicative of predominantly algal-derived organic contribution to the sediment. The finding of a generally low C:N ratio throughout the section is reasonable, as this is the product of fluvial

deposition, where algae is likely to dominate the organic matter (Meyers, 1994). However, the slightly higher C:N values, seen in the initial suspended-load channel fill sequence and channel deposits 1 and 5, indicate some input from terrestrial plants.

The dominant plant in Permian wetlands was the gymnosperm *Glossopteris*, and fossilized specimens of this taxon are reported in the New Wapadsberg section (Prevec *et al*., 2010). The presence of this taxon in the stratigraphy suggests that *Glossopteris* is a likely source for the terrestrial plant inputs to these fluvial deposits. This input, however, would be limited as, with the exception of three points in the lower and middle sections, the C:N values in most samples throughout the section range from about 5 to about 8, indicating minimal terrestrial organic inputs. No sample had a C:N ratio higher than 15, which is indicative of a mixed contribution. This indicates that there was no large-scale shift in organic source throughout the section, with algae being consistently the dominant contributor.

A fluvial channel fill with an algal signature would likely have been one without significant overhanging vegetation or transport of terrestrial organic material from distant upstream sites (Allan and Castillo, 2007). The high width:depth (about 10:1) ratio of the Wapadsberg Pass section would also allow for extensive algal growth in the exposed center of a recently abandoned channel, where lake-like conditions would dominate. The expansive width of this system also provides the potential for a difference in C:N ratio for sediment at different distances from the channel margins. Samples originating from near the edge of the channel would be more likely to have a terrestrial input than those in the center (Kaushal and Binford, 1999). In the Wapadsberg Pass channels, all of samples that have C:N values >10 were collected from areas closer to a channel bank than the majority of samples. Most samples were collected from near the middle of a paleochannel (Fig. 12), and their low TOC:TON values confirm the

interpretation that terrestrial input from the channel margins did not reach the mid-channel sediments. The consistency of the samples in the upper third of the section may be explained by the fact that all samples were taken from well-developed bedforms, which would likely have limited terrestrial organic inputs. The observed C:N pattern is likely the result of the channel location from which samples were taken and not a complete loss of *Glossopteris* input in the upper section.

The TOC:TON values recorded from throughout the Wapadsberg Pass section indicate that organic matter contribution originated from within wide, routinely abandoned channels, which were bounded by a vegetative margin. There is no evidence of a change in this river character based on the C:N signature. Similarly, there is no evidence of a widespread terrestrial plant die-off, as this would likely result in a severe increase in C:N values, resulting from the decay of plant material and the leaching of these organics into the river system (Kaushal and Binford, 1999).

4.4. Sandstone Petrography Analysis

Grain Size

The Wapadsberg Pass section is an overall fine-grained system, with a limited range in clasts sizes between bedload and suspension-load facies. The bedload sandstones are moderately to poorly sorted, and generally negatively skewed, indicating the predominance of finer grains. Wacke sandstones are limited to the base of each channel iteration, with overlying sediments of varying thickness following the slope of erosive bases. These represent the bedload deposits.

The fine-grained nature of the bedload sand component is a reflection of the energy of the river system. This was likely a fairly low energy system, as fine to very fine sand grains dominate the bedload deposits. The skewness in the sandstones is an indication that fine grains

were preferentially sorted over coarse grains (Folk, 1966). This indicates that finer grains could be carried by the system with more regularity than coarse grains. However, it is important to note that there is little context for this river system, given that all that can be seen is a preserved cross-tangential section. If source material had all been broken down to fine/medium size grains by the time it reached this stretch of river, then that would clearly be all that was preserved. Hence, a fine average grain size and a negative skewness do not indicate that larger clasts could not be transported, only that they were not transported to this isolated location in the river system.

In general, the Wapadsberg sandstone units occupy a similar position within a fluvial architectural model to the Ss lithofacies described by Miall (1996) as "scour-fill sand" that drapes over a basal bounding surface. These Ss units are poorly sorted and interpreted as the result of rapid deposition of the bedload (Miall, 1996). However, the fine sandstone lithofacies from the Wapadsberg section differs from the Ss lithofacies in that the latter is described as primarily a coarse to very coarse grained sand. It is plausible that these two facies are the result of a similar process, just formed by different energy regimes in different river systems.

Mineralogy

Sandstones from the Wapadsberg Pass section are generally quartz or lithic dominated wackes (>90% quartz or >10% lithics, respectively), with low feldspar content (1-8%). Quartz and feldspar in sedimentary rocks are derived commonly from granites and gniesses; however, the nature of the crystals can help to narrow down the source-rock type. Quartz in the Wapadsberg Pass sandstones is typically moncrystalline and without inclusions, indicating a likely source of volcanic igneous rocks (Tucker, 1991). The presence of undulose extinction, although once thought to be characteristic of metamorphic grains, often can be found in volcanically-derived quartz grains (Tucker, 1991).

Feldspar grains are predominantly orthoclase. The K-feldspars are more common in sandstones than plagioclase due to a greater chemical stability. Limited quantities of feldspar grains may be the result of a lower mechanical and chemical stability relative to quartz; hence, diagenetic alteration is common and may distort the percentages seen in ancient samples (Tucker, 1991).

A predominantly Quartz-feldspar mineralogy is indicative of a volcanic source material for these sandstones; however, the significant lithic component indicates that grains were not derived from a continental basement. Grains derived from this setting would likely be predominantly quartz and feldspar, with only a small proportion of lithic fragments (Tucker, 1991). Lithic fragments commonly are derived from mountain belts or rapidly-uplifting volcanic areas, where erosion will make available a more diverse set of rock fragments and minerals (Tucker, 1991). Given the relative abundances and characteristics of quartz, feldspar, and lithic grains in the Wapadsberg Pass samples, sediments were likely sourced from a mountain-belt composed of predominantly igneous rocks. This fits with the understanding that the Karoo Basin constituted a closed basin in the Latest Permian, bounded by upland areas on all sides, and with the Cape Fold Belt to the southwest (Smith *et al.*, 1993; Johnson *et al.*, 2006; Rubidge *et al.*, 2012).

4.5 Analysis of Middle and Upper Section Channel Bases/Barforms

Analysis of the thicker (>2 m) and coarser basal sequences in the middle and upper parts of the stratigraphic section (Fig. 10) provides information about changes in grain size, grain sorting, and mineralogy in and among bedforms. These sequences form the basalmost deposits of channels 5, 6, and 7, and are referred to as barforms 1, 2, and 3, respectively (Fig. 10). The bottom of barform 1 (middle section @ ~24 m) shows a significant bias towards fine grains

(negatively skewed), with a dominance of quartz minerals (Sample 17.01.01). This sample is similar in sorting and mineralogical features to the one taken from 2500 cm, in the middle of the first barform, (Sample 17.01.02). The base of barform 2 (@ ~30 m) has a more symmetrical grain size distribution,a higher proportion of lithic grains (Sample 18.01.14), and is most similar to the top of the first barform (Sample 18.01.17). Figure 9 shows that the similar pairs of samples are from roughly the same location within a bed; samples 17.01.01 and 17.01.02 are from the base of beds and samples 18.01.14 and 18.01.17 are from the middle/top of beds. This indicates a change in grain characteristics throughout individual beds, with the same changes associated with each bed. There does not seem to be a significant change in grain size or mineralogy between different beds.

Changes within Beds

Barform 1, which is found in the Middle Section of the stratigraphic section, consists of two 1-m beds, and shows a general pattern of coarsening upwards throughout the unit. The lithology transitions from sandy coarse siltstone to silty sandstone with an increase in the sand:silt proportions in each sample. Based on the 2 sandstone samples from the upper bed of this unit (17.01.02; 18.01.17) there are fewer fine grains and a higher lithic content at the top of the bed. A coarsening in grain size may indicate increased energy of the system. However, because this grain size change is on the scale of a few micrometers, and is more a reflection of the ratio of sand:silt, it is likely that coarsening resulted from natural variation in river velocity over time.

Barforms 2 and 3 are located in the Upper Section of the stratigraphy and show a similar pattern in grain size variability. The main erosional surface is underlain by slightly finer material than the sediment found at the base of the barform. The coarsest part of the barform is at the

base, followed by a fining upward sequence, as evidenced by a decreasing sand:silt ratio. These two units show a different pattern than the stratigraphically lower 1st barform in the Middle part of the stratigraphy. A decrease in sand:silt ratio indicates a slight change in river velocity over time. This grain size change is not known to be reflected in mineralogy, which is unknown. This is because barform 2 consists of only sandy coarse silt and barform 3 was too metamorphically altered by an adjacent dolorite intrusion for mineralogy to be determined.

The changes documented in the bedforms of the middle and upper sections are relatively minimal and not indicative of large-scale processes. Changes in grain size distribution from barform to barform can be the result of river flow variability. The general mineralogy, sorting, and grain size are fairly consistent, and don't reflect major changes in river movement or source material during the bedload deposition. However, these changes may result from the progression of flow differences as a river erodes a channel, migrates away, and the abandoned channel is filled in.

4.6. Channel System Morphology and Migration

Morphology

The Wapadsberg Pass section is interpreted to include 8 iterations of a single meandering river channel system, the history of which is recorded over a composite stratigraphic thickness of 40 m. Each channel iteration is underlain by and erosive 5th order bounding surface (Miall, 1996). This channel system is relatively wide (>40 m) and shallow (<6 m), with a depositional dip of about 4° indicative of the slope of the channel margins. This dip is reduced to nearly horizontal bedding within the barform, which marks the basal deposit of the first channel in this section at ~10.3 m. This is the only place in the section where a channel bottom can be definitively identified (Fig. 11; Section A).

A lack of change in bedding dip across the remainder of the section is indicative of a consistent channel structure, likely stabilized and contained by bank vegetation. This indicates that no significant change in channel morphology occured throughout the section; this remains a meandering paleochannel. Most of what is seen in the section is the SE dipping margin of the channel system (Figs. 5, 11, 12). The remainder of the cross section for each channel is cut off by the subsequent stratigraphically higher iteration (Fig. 12).

Channel margins do not show a steepening to the NW or evidence of significantly more erosion on this side, an indication that the section does not display a cut bank. Additionally, there is no evidence of any extensive sandbar development on the NW bank (Fig. 11) and the dip is likely too steep to constitute deposition in a point bar. Because of this, the section most likely does not represent a view of a meander bend, where differences in flow velocity would cause the development of erosional cutbanks and depositional point bars. Rather, the section likely provides a nearly cross-sectional view of the relatively straight stretch of river between meander bends, where there is less differential flow and no extreme erosion or deposition on either bank (Fig. 12A).

Migration across the Landscape

One defining characteristic of a meandering channel regime is its migration across a floodplain over time. This movement has been modeled and simulated for both modern and ancient rivers (*eg.,* Meakin *et al.,* 1996; Burge and Smith, 1999; Nicoll and Hicken, 2010). However, the numerous unknown parameters and limited availability of outcrop at Wapadsberg Pass prevent the reconstruction of a definitive migration pattern in this paleo-system. The stacked and offset nature of the Wapadsberg Pass stratigraphy provides evidence of channel migration over time. Combined with this is floodplain aggradation that accounts for the fact that

each subsequent channel is located stratigraphically higher than the previous. Channel bases are fairly definitive, as marked by erosional bounding surfaces, with noticeably coarser sediment above and finer material beneath bounding surfaces. There are instances of thin, coarsening upward intervals below channel bases in 5 of the channels. This indicates that each channel must have been abandoned, and the next iteration to move back eroded into the sediment from the previous fill complex. The fluvial deposits at Wapadsberg Pass are not interpreted as a slight continuous movement of one channel iteration, for this would likely be manifested as a gradual lateral change in lithofacies, not distinct sequences marked by erosive bases. A visual model for the migration of the small section of the river system exposed at Wapadsberg Pass is provided in Figure 12A. This model shows abandonment of meander loops, followed by the development of new meander bends slightly downstream from the previous and with approximately the same lateral extent. The offset of each successive iteration of the channel in the downstream direction is consistent with models of meandering systems that show a gradual shift in meander bend towards the downstream direction (Burge and Smith, 1999; Nicoll and Hicken, 2010). This forward progression in meander bends over time could account for the fact that each successive channel in the Wapadsberg Pass section is offset to the SE, not stacked directly on top of the previous.

The spatial regularity of the channel forms may be the result of channel confinement, which would have limited the lateral extent of the meander bends, constraining the system. Nicoll and Hicken (2010) and Burge and Smith (1999) describe two confined river systems that result in a very regular meander migration. These authors found that meandering channels in a confined valley routinely impinged upon the valley margin, meaning that the extent of lateral migration was consistent over time (Burge and Smith, 1999). This allowed for a predictable

fluvial morphology, where meanders returned to roughly the same location as previous iterations of the channel (Burge and Smith, 1999; Nicoll and Hicken, 2010). The consistency of channel movement in the Wapadsberg pass system is not necessarily evidence of a dominant confining structure; however, confinement is one explanation for why a more chaotic river migration is not seen in this system. The direction of channel accretion and bank characteristics in the Wapadsberg Pass section indicate that this cross section is from approximately midway between two meander bends (Fig. 12A). If the channels were abandoned via cut offs of the main channel long enough for vegetation to take root in the newly deposited channel-fill sediment, evidence of this is not seen in the TOC:TON values of the samples collected. This could either be due to the fact that migration occurred fast enough that the abandoned areas were not vegetated or that this evidence was removed by the erosion of subsequent channels.

4.7. Comparison to Other Karoo Studies

Although the Karoo Basin has been a critical area for studying the Permian-Triassic Boundary on land, there is still debate about the details and interpretations of the lithostratigraphy surrounding the PTB, and how this relates to the biostratigraphy. This study provides new information about uppermost Permian stratigraphy in the context of fluvial systems preceding the PTB, as recognized based on vertebrate biostratigraphy (Ward *et al.*, 2005; Smith and Botha-Brink, 2014). Permian-Triassic river systems first were described by Smith (1995) as transitioning from high-sinuosity meandering to braided across the boundary, a model reiterated by Ward *et al.* (2000) and Smith and Botha-Brink (2014). The changeover in fluvial architectures is reported to be associated with a pattern of climate change to a more arid landscape, accompanied by vegetation die-off and vertebrate extinction (Smith, 1995; Ward *et al.* 2000; Ward *et al.*, 2005; Smith and Botha-Brink, 2014).

The New Wapadsberg Pass section along the R61 highway lies just below the vertebrate-defined PTB, as recognized at Old Wapadsberg Pass (Ward *et al.,* 2005; Prevec *et al.,* 2010; Gastaldo *et al.,* 2014) providing an important section for comparison with the presently accepted model of changing fluvial style in response to the event. Based on the Smith (1995) and Ward *et al.* (2000) model, and the *Glossopteris* bed of known stratigraphic position (Prevec *et al*., 2010), the fluvial regimes outcropped along the Wapadsberg Pass section can be placed into the zone of high-sinuosity meandering rivers, characteristic of the latest Permian. The studied fluvial system fits this proposed scheme, as evidence supports an interpretation as a meandering system with repeated channel abandonment and bend migration. The second phase of the Smith (1995) model, that occurs immediately prior to the extinction event, envisions a transition to lower sinuosity rivers that eventually are replaced by Early Triassic braid-plains. Braid-plain development occurs within 30 m above the PTB (Smith, 1995). The transition to braid-plains is reported to have been driven by a tectonic pulse that increased sediment load, as well as loss of bank-stabilizing vegetation due to climate change (Smith, 1995; Ward *et al*., 2000). The transition seen in the Wapadsberg Pass system (from low bedload to high bedload proportions) could be explained by a pulse of uplift that increased sediment supply from the source area. However, it is unlikely that such an orogenic pulse would have occurred fast enough to alter sediment supply over the life-history of a single meandering channel system. A more likely explanation for increased sediment loads is a more regular water flow that was capable of eroding, transporting, and depositing a larger bedload supply at the Wapadsberg Pass site prior to channel abandonment.

Smith (1995) and Ward *et al.* (2000) do not suggest that there was a transition in fluvial style before the PTB; however, this interpretation is recently modified by Smith and Botha-Brink

(2014). They suggest a multi-phase extinction of vertebrate taxa was accompanied by various climatic changes that are reflected in the rock record. The onset of increased seasonality and less predictable rainfall patterns now is interpreted to begin ~45 m below the PTB. Associated with increasing seasonality was a lowering of the water table (Smith and Botha-Brink, 2014), which can be identified in the rock record by evaporitic gypsum rosettes and shallow rooting. Gastaldo *et al.* (2014) report evidence of warm and wet conditions in two paleosol horizons approximately 70 m below the PTB at Old Wapadsberg Pass. They also report that calcite $\delta^{13}C$ values from calcareous nodules for most of the Wapadsberg Pass section are consistent with calcite precipitation under saturated soil conditions. These data conflict with the Smith and Botha-Brink (2014) assessment that the lowering of the water table began ~45 m below the PTB, exposing soils to atmospheric CO2 that was incorporated into nodules. Under their model, the stable isotope geochemistry of nodules associated with the stratigraphic section of the current study would have to be different than what is reported by Gastaldo *et al.* (2014).

According to the Smith and Botha-Brink (2014) model, increasingly less reliable rainfall resulted in vegetation die-off by the time of the PTB, and monsoon-like conditions resulted in scouring of floodplains. Evidence of a loss of bank-stabilizing vegetation or floodplain scouring is not seen at the Wapadsberg Pass section. Rather, this section contains a cohesive meandering channel system that is likely stabilized by bank vegetation throughout the stratigraphy. These observations suggest that current models for the timing of braid-plain development may not be accurate basin-wide. And, there is at least one study that reports *Glossopteris* in the early Triassic of Antarctica (McManus *et al.,* 2002). Hence, it is plausible that bank-stabilization and meandering river channels persisted through the late Permian and potentially into the early Triassic.

The characteristics of the Wapadsberg Pass fluvial system call into question some aspects of the proposed timing for fluvial transition in the Karoo Basin. Additionally, a recent study recovered a single earliest Triassic-aged zircon grain from New Wapadsberg Pass, indicating that a reevaluation of fluvial transitions relative to both stratigraphic and date-based chronologies may be necessary. The date came from an ash layer at ~10 m height in the study section and was 252.0 ± 0.5 Ma (unpublished results). Although more data would be needed to substantiate this result, this indicates a possibility that the Wapadsberg Pass section may be slightly younger than is currently assumed. Further research would need to be done, but if this section is Triassic aged, that would have implications not only for the timing of fluvial transitions, but also for the positioning of the PTB and the accuracy of the vertebrate-defined boundary.

4.8. Paleoenvironmental Implications

Although debate exists about the earliest Triassic climate, the most common model for PTB climate change implicates a transition from humid to more arid conditions (Smith and Botha-Brink, 2014). The reported climatic change was accompanied by a die-off of a significant amount of vegetation and many vertebrate species (Smith and Botha-Brink, 2014). The cohesiveness of channels in the Wapadsberg Pass river system does not indicate any loss of bank-stabilization. This indicates that at this stratigraphic location of ~50-10 m below the PTB (Gastaldo *et al.*, 2014), which is in the range of extinction phase 1 (45-30 m below PTB) and extinction phase 2 (20-0 m below PTB) as defined by Smith and Both-Brink (2014), vegetation die-off had not yet occurred and climate change either had not happened yet or had not yet affected channel-margin plants. Increased bedload sediments may have been the result of (1) more water carrying capacity of coarser sediment or (2) increased sediment load. The first scenario would contradict many of the models that interpret much drier conditions across the

boundary, lasting into the early Triassic (Ward *et al*., 2000, 2005; Smith and Botha-Brink, 2014). The second scenario may correlate with a known tectonic pulse in the early Triassic (Smith, 1995), indicating that meandering rivers of sufficient energy to carry thick (>2 m) sequences of bedload may have persisted into the Triassic. The system exposed at the Wapadsberg Pass section is indicative of an environment that contained an adequate supply of water to feed a continually migrating, large river, with successful bank vegetation capable of containing the channel.

5. CONCLUSIONS

The Wapadsberg Pass fluvial systems provide an additional tool for interpreting climate change leading up to the PTB in the Karoo Basin. By providing a cross-sectional view of an en echelon stacked channel system, this outcrop shows changes in both vertical and lateral sedimentation patterns in the latest Permian. The fluvial system shows a general transition from low bedload- channel to high bedload–channel deposits over a stratigraphic distance of 40 meters. The laterally adjacent positions of successive river channels is interpreted as a meandering channel system, where channel bends were routinely abandoned, filled with sediment, and later eroded into by a subsequent iteration of the channel. There is no evidence of a change in river morphology in this section. Additionally, evidence of a mass die-off of bank-stabilizing vegetation or an increasingly arid climate is not found, although models for these patterns have been presented (Smith, 1995; Ward *et al.*, 2000; 2005; Smith and Botha-Brink, 2014). Climate change across the PTB is still widely debated; therefore, additional studies of climatically-controlled fluvial systems could be used to enhance and solidify climate models for this extinction event.

LITERATURE CITED

Allan, J.D., and Castillo, M.M., 2007, Stream Ecology: Springer, Dordrecht, The Netherlands, 436 p.

Angielczyk, K.D., and Kurkin, A.A., 2003, Has the utility of *Dicynodon* for Late Permian terrestrial biostratigraphy been overstated?: Geology, v. 31, p. 363-366.

Arche, A., and López-Gómez, J., 2005, Sudden changes in fluvial style across the Permian-Triassic in the eastern Iberian Ranges, Spain: Analysis of possible causes: Palaeogeography, Palaeoclimatology, Palaeoecology, v. 229, p. 104-126.

Bangert, B., Stollhofen, H., Lorenz, V., and Armstrong, R., 1999, The geochronology and significance of ash-fall tuffs in the glaciogenic Carboniferous-Permian Dwyka Group of Namibia and South Africa: Journal of African Earth Sciences, v. 29, p. 33-49.

Benton, M.J. and Newall, A.J., 2014, Impacts of global warming on Permo-Triassic terrestrial ecosystems: Gondwana Research, v. 25, p. 1308-1337.

Berner, R.A., 2005, The carbon and sulfur cycles and atmospheric oxygen from the middle Permian to middle Triassic: Geochimica et Cosmochimica Acta, v. 69, p. 3211-3217.

Botha, J., and Smith, R.M.H., 2007, *Lystrosaurus* species composition across the Permo-Triassic Boundary in the Karoo Basin of South Africa: Lethaia, v. 40, p. 125-137.

Burge, L.M., and Smith, D.G., 1999, Confined meandering river eddy accretions: sedimentology, channel geometry and depositional processes: Special Publications of the International Association of Sedimentologists, v. 28, p. 113-130.

Burgess, S.D., Bowring, S., and Shen, S., 2014, High-precision timeline for the Earth's most severe extinction: PNAS, doi: 10.1073/pnas.1317692111.

Catuneanu, O., Wopfner, H., Eriksson, P.G., Cairncross, B., Rubidge, B.S., Smith, R.M.H., and

Hancox, P.J., 2005, The Karoo basins of south-central Africa: Journal of African Earth Sciences, v. 43, p. 211-253.

Coney, L., 2005, Mineralogical-geochemical investigation of two sections across the Permian-Triassic Boundary in the continental realm of the southern Karoo Basin, South Africa: unpublished M.Sc. Thesis, University of Witwatersrand, Johannesburg, South Africa, 177 p.

Coney, L., Reimold, W.U., Hancox, J.P., Mader, D., Koeberl, C., McDonald, I., Stuck, U., Vajda, V., and Kamo, S.L., 2007, Geochemical and mineralogical investigation of the Permian-Triassic boundary in the continental realm of the southern Karoo Basin, South Africa: Paleoworld, v. 16, p. 67–104.

De Kock, M.O., and Kirschvink, J.L., 2004, Paleomagnetic constraints on the Permian-Triassic Boundary in the terrestrial strata of the Karoo Supergroup, South Africa: Implications for causes of the end-Permian extinction event: Gondwana Research, v. 7, p. 175-183.

De Wit, M.J., Ghosh, J.G., de Villiers, S., Rakotosolofo, N., Alexander, J., Tripathi, A., and Looy, C., 2002, Multiple organic carbon isotope reversals across the Permo-Triassic boundary of terrestrial Gondwana 131 sequences: Clues to extinction patterns and delayed ecosystem recovery: Journal of Geology, v. 110, p. 227-240.

Erwin, D.H., 1994, The Permo-Triassic extinction: Nature, v. 367, p. 231-236.

Fildani, A., Drinkwater, N.J., Weislogel, A., McHargue, T., Hodgson, D.M., and Flint, S.S., 2007, Age controls on the Tanqua and Laingsburg deep-water systems: new insights on the evolution and sedimentary fill of the Karoo Basin, South Africa: Journal of Sedimentary Research, v. 77, p. 901-908.

Folk, R.L., 1966, A review of grain-size parameters: Sedimentology, v. 6, p. 73-93.

Gastaldo, R.A., Adendorff, R., Bamford, M., Labandeira, C.C., Neveling, J., and Sims, H., 2005, Taphonomic trends of macrofloral assemblages across the Permian-Triassic Boundary, Karoo Basin, South Africa: Palaios, v. 20, p. 479-497.

Gastaldo, R.A., Neveling, J., Clark, C.K., and Newbury, S.S., 2009, The terrestrial Permian-Triassic boundary event bed is a non-event: Geology, v. 37, p. 199-202.

Gastaldo, R.A., and Neveling, J., 2012, The terrestrial Permian-Triassic boundary event is a nonevent: REPLY: Geology, v. 40, p. e257, doi:10.1130/G32975Y.1

Gastaldo, R.A., Pludow, B.A., Neveling, J., 2013, Mud aggregates from the Katberg Formation, South Africa: Additional evidence for early Triassic degradational landscapes: Journal of Sedimentary Research, v. 83, p. 531-540.

Gastaldo, R.A., Knight, C.L., Neveling, J., and Tabor, N.J., 2014, Latest Permian paleosols from Wapadsberg Pass, South Africa: Implications for Changsingian climate: Geological Society of America Bulletin, doi:10.1130/B30887.1.

Glen, J.M.G., Nomade, S., Lyons, J.J., Metcalfe, I., Mundil, R., and Renne, P.R., 2009, Magnetostratigraphic correlations of Permian-Triassic marine-to-terrestrial sections from China: Journal of Asian Earth Sciences, v. 36, p. 521-540.

Hancox, P.J., and Rubidge, B.S., 2001, Breakthroughs in biodiversity, biogeography, biostratigraphy, and basin analysis of the Beaufort Group: Journal of African Earth Sciences, v. 33, p. 563-577.

Koeberl, C., and MacLeod, K.G. (eds.), 2002, Permian-Triassic boundary in the northwest Karoo Basin: Current stratigraphic placement, implications for basin development models, and search for evidence of impact: In Catastrophic Events and Mass Extinctions: Impacts and Beyond Geological Society of America Special Paper, v. 356, p. 429-444.

Heller, F., Haihong, C., Dobson, J., and Haag, M., 1995, Permian-Triassic magnetostratigraphy – new results from South China: Physics of the Earth and Planetary Interiors, v. 89, p. 281-295.

Holzförster, F., 2007, Lithology and depositional environments of the Lower Jurassic Clarens Formation in the Eastern Cape, South Africa: South African Journal of Geology, v. 110, p. 543-560.

Johnson, M.R., 1976, Stratigraphy and sedimentology of the Cape and Karoo Sequences in the Eastern Cape Province: Doctoral Thesis, Department of Geology, Rhodes University, Gramstown.

Johnson, M.R. (ed.), 1994, Lexicon of South African Stratigraphy. Part 1: Phanerozoic Units: Council for Geoscience, South Africa, 56 p.

Johnson, M.R., Van Vuuren, C.J., Hegenberger, W.F., Key, R., and Shoko, U., 1996, Stratigraphy of the Karoo Supergroup in southern Africa: An overview: Journal of Africa Earth Sciences, v. 23, p. 3-15.

Johnson, M.R., van Vuuren, C.J., Visser, J.N.J., Cole, D.I., Wickens, H. de V., Christie, A.D.M., Roberts, D.L., and Brandl, G., 2006, Sedimentary rocks of the Karoo Supergroup: *in* Johnson, M.R., Anhaeusserm, C.R., and Thomas, R.J., Eds., The Geology of South Africa: Geological Society of South Africa, Johanesburg, Council for Geoscience, Pretoria, p. 461-479; 492-495.

Jordaan, M.J., 1981, The Ecca-Beaufort transition in the Western parts of the Karoo Basin: Transactions of the Geological Society of South Africa, v. 84, p. 19-25.

Jourdan, F., Féraud, G., Bertrand, H., Kampunzu, A.B., Tshoso, G., Watkeys, M.K., and Le Gall,

B., 2005, Karoo large igneous province: Brevity, origin, and relation to mass extinction questioned by new $^{40}Ar/^{39}Ar$ age data: Geology, v. 33, p. 745-748.

Jourdan, F., Féraud, G., Bertrand, H., Watkeys, M.K., and Renne, P.R., 2007, Distinct brief major events in the Karoo large igneous province clarified by new $^{40}Ar/^{39}Ar$ ages on the Lesotho basalts: Lithos, v. 98, p. 195-209.

Kapupu, C., Gastaldo, R.A., and Neveling, J., 2010, The lithological characterization of a Middle Permian deltaic distributary channel, in the Karoo Basin, South Africa: Geological Society of America Abstracts with Programs, v. 42, p. 428.

Kaushal, S., and Binford, M.W., 1999, Relationship between C:N ratios of lake sediments, organic matter sources, and historical deforestation in Lake Pleasant, Massachusetts, USA: Journal of Paleolimnology, v. 22, p. 439-442.

Kiehl, J.T., and Shields, C.A., 2005, Climate simulation of the latest Permian: Implications for mass extinction: Geology, v. 33, p. 757-760.

King, G.M., 1990, Dicynodonts and the end Permian event: Palaeontologia Africana, v. 27, p. 31-39.

Korte, C., and Kozur, H.W., 2010, Carbon isotope stratigraphy across the Permian-Triassic boundary: a review: Journal of Asian Earth Sciences, v. 39, p. 215-235.

Kozur, H.W., 1998, Some aspects of the Permian-Triassic boundary (PTB) and the possible cause for the biotic crisis around this boundary: Palaeogeography, Palaeoclimatology, Palaeoecology, v. 143, p. 227-272.

Lindeque, A., De Wit, M.J., Ryberg, T., Weber, M., and Chevallier, L., 2011, Deep crustal

profile across the southern Karoo Basin and Beattie magnetic anomaly, South Africa: An integrated interpretation with tectonic implications: South African Journal of Geology, v. 114, p. 265-292.

Lucas, S.G., 2009, Timing and magnitude of tetrapod extinctions across the Permo-Triassic boundary: Journal of Asian Earth Sciences, v. 36, p. 491-502.

MacLeod, K.G., Smith, R.M.H., Koch, P.L., and Ward, P.D., 2000, Timing of mammal-like reptile extinctions across the Permian-Triassic boundary in South Africa: Geology, v. 28, p. 227-230.

McManus, H.A, Taylor, E.L., Taylor, T.N., and Collinson, J.W., 2002, A petrified *Glossopteris* flora from the Collinson Ridge, central Transantarctic Mountains: Late Permian or Early Triassic?: Review of Palaeobotany and Palynology, v. 120, p. 233-246.

Meakin, P., Sun, T., Jossang, T., and Schwarz, K., 1996, A simulation model for meandering rivers and their associated sedimentary environments: Physica A, v. 233, p. 606-618.

Metcalfe, I., and Isozaki, Y., 2009, Current perspectives on the Permian-Triassic Boundary and end-Permian mass extinction: Preface: Journal of Asian Earth Sciences, v. 36, p. 407-412.

Meyers, P.A., 1994, Preservation of elemental and isotopic identification of sedimentary organic matter: Chemical Geology, v. 114, p. 289-302.

Miall, A.D., 1996, The Geology of Fluvial Deposits: Springer-Verlag, Italy, 582 p.

Michaelsen, P., 2002, Mass extinction of peat-forming plants and the effect on fluvial styles across the Permian-Triassic boundary, northern Bowen Basin, Australia: Palaeogeography, Palaeoclimatology, Palaeoecology, v. 179, p. 173-188.

Montenegro, A., Spence, P., Meissner, K.J., Eby, M., Melchin, M.J., and Johnston, S.T., 2011,

Climate simulations of the Permian-Triassic boundary: Ocean acidification and the extinction event: Paleoceanography, v. 26, PA3207.

Nicoll, T.J., and Hickin, E.J., 2010, Planform geometry and channel migration of confined meandering rivers on the Canadian prairies: Geomorphology, v. 116, p. 37-47.

Pace, D.W., Gastaldo, R.A., and Neveling, J., 2009, Aggradational and Degradational Landscapes in the Early Triassic of the Karoo Basin and Evidence for Dramatic Climate Shifts Following the P/Tr Event: Journal of Sedimentary Research, v. 79, p. 276-291.

Payne, J.L., and Clapham, M.E., 2012, End-Permian mass extinction in the oceans: An ancient analog for the Twenty-First Century: Annual Reviews of Earth and Planetary Science Letters, v. 40, p. 89–111 doi: 10.1146/annurev-earth-042711-105329.

Prevec, R., Gastaldo, R.A., Neveling, J., Reid, S.B., and Looy, C.V., 2010, An autochthonous Glossoperid flora with Latest Permian palynomorphs from the *Dicynodon* Assemblage Zone of the southern Karoo Basin, South Africa: Palaeogeography, Palaeoclimatology, Palaeoecology, v., 292, p. 381-408. doi: 10.1016.

Retallack, G.J., 1995, Permian-Triassic crisis on land: Science, v. 267, p. 77-80.

Retallack, G.J., Smith, R.M.H., and Ward, P.D., 2003, Vertebrate extinction across Permian-Triassic boundary in Karoo Basin, South Africa: Geological Society of America Bulletin, v. 115, p. 1133-1152.

Reid, S.B., Gastaldo, R.A., Neveling, J., and Tabor, N., 2007, Fluvial systems and carbonate nodules reveal Late Permian climate change at Wapadsberg Pass, Eastern Cape Province, South Africa: Geological Society of America Abstracts with Programs, v. 39, p. 85.

Rubidge, B.S. (ed.), 1995, Biostratigraphy of the Beaufort Group (Karoo Supergroup), South Africa: South African Committee for Stratigraphy Biostratigraphic Series 1, 45 p.

Rubidge, B.S., 2005, Re-uniting lost continents– Fossil reptiles from the ancient Karoo and their wanderlust: South African Journal of Geology, v. 108, p. 135-172.

Rubidge, B.S., Modesto, S., Sidor, C., and Welman, J., 1999, Eunotosaurus africanus from the Ecca-Beaufort contact in Northern Cape Province, South Africa: South African Journal of Science, v. 95, p. 553-555.

Rubidge, B.S., Hancox, P.J., and Catuneanu, O., 2000, Sequence analysis of the Ecca-Beaufort contact in the southern Karoo of South Africa: South African Journal of Geology, v. 103, p. 81-96.

Rubidge, B.S., Hancox, P.J., and Mason, R., 2012, Waterford Formation in the south-eastern Karoo: Implications for basin development: South African Journal of Science, v. 2., p. 285-288.

Rubidge, B.S., Erwin, D.H., Ramezani, J., Bowring, S.A., and de Klerk, W.J., 2013, High-precision temporal calibration of Late Permian vertebrate biostratigraphy: U-Pb zircon constraints from the Karoo Supergroup, South Africa: Geology, v. 41, p. 363-366.

Smith, R.M.H., 1980, The lithology, sedimentology and Taphonomy of flood-plain deposits of the Lower Beaufort (Adelaide Subgroup) strata near Beaufort West: Transactions of the Geological Society of South Africa, v. 83, p. 399-413.

Smith, R.M.H., 1990, Alluvial paleosols and pedofacies sequences in the Permian Lower Beaufort of the southwestern Karoo Basin, South Africa: Journal of Sedimentary Petrology, v. 60, p. 258-276.

Smith, R.M.H., 1995, Changing fluvial environments across the Permian-Triassic boundary in the Karoo Basin, South Africa, and possible causes of tetrapod extinctions: Palaeogeography, Palaeoclimatology, Palaeoecology, v. 117, p. 81-104.

Smith, R.M.H., and Ward, P.D., 2001, Patterns of vertebrate extinctions across an event bed at the Permian-Triassic boundary in the Karoo Basin of South Africa: Geology, v. 29, p. 1147–1150.

Smith, R.M.H., and Botha, J., 2005, The recovery of terrestrial vertebrate diversity in the South African Karoo Basin after the end-Permian extinction: Comptes Rendus-Palevol, v. 4, p. 555-568.

Smith, R.M.H., and Botha-Brink, J., 2014, Anatomy of a mass extinction: Sedimentological and taphonomic evidence for the drought-induced die-offs at the Permian-Triassic boundary in the main Karoo Basin, South Africa: Palaeogeography, Palaeclimatology, and Palaeoecology, v. 393, p. 99-118.

Smith, R.M.H., Eriksson, P. G., and Botha, W. J., 1993, A review of the stratigraphy and sedimentary environments of the Karoo-aged basins of Southern Africa: Journal of African Earth Sciences, v. 16, p. 143-169.

South African Committee for Stratigraphy (SACS) (Compiler L.E. Kent), 1980, Stratigraphy of South Africa, Part I. Lithostratigraphy of the Republic of South Africa, South Waest Africa/Namibia, and the Republics of Bophuthatswana, Transkei, and Venda: Geological Survey South Africa Handbook v. 8, 690 p.

Stanley, S.M., 1988, Climatic cooling and mass extinction of Paleozoic reef communities: Palaios, v. 3, p. 228-232.

Stear, W.M., 1983, Morphological characteristics of ephemeral stream channel and overbank splay sandstone bodies in the Permian Lower Beaufort Group, Karoo Basin, South Africa: Special Publication of the International Association of Sedimentologists, v. 6, p. 405-420.

Steiner, M.B., Ogg, J., Zhang, Z., and Sun, S., 1989, The late Permian/early Triassic magnetic polarity time scale and plate motions of south China: Journal of Geophysical Research, v. 94, p. 7343-7363.

Steiner, M.B., Eshet, Y., Rampino, M.R,. and Schwindt, D.M., 2003, Fungal abundance spike and the Permian-Triassic boundary in the Karoo Supergroup (South Africa): Palaeogeography, Palaeoclimatology, Palaeoecology, v. 194, p. 405-414.

Talbot, M.R., and Kelts, K., 1986, Primary and diagenetic carbonates in the anoxic sediments of Lake Bosumtwi, Ghana: Geology, v. 14, p. 912-916.

Taylor, G.K., Tucker, C., Twitchett, R.J., Kearsey, T., Benton, M.J., Newell, A.J., Surkov, M.V., and Tverdokhlebov, V.P., 2009, Magnetostratigraphy of Permian-Triassic boundary sequences in the Cis-Urals, Russia: No evidence for a major temporal hiatus: Earth and Planetary Science Letters, v. 281, p. 36-47.

Thackeray, J.F., van der Merwe, N.J., Lee-Thorpe, J.A., Sillen, A., Lanham, J.L., Smith, R.M.H., Keyser, A. and Monteiro, P.M.S., 1990, Changes in carbon isotope ratios in the Late Permian recorded in therapsid tooth apatite: Nature, v. 347, p. 751-753.

Tucker, M.E., 1991, Sedimentary Petrology: Blackwell Scientific Publications, London, Great Britain, 260 p.

Twitchett, R.J., 2007, Climate change across the Permian-Triassic Boundary: Geological Society Special Publication, p. 191-200.

Twitchett, R.J., Looy, C.V., Morante, R., Visscher, H., and Wignall, P.B., 2001, Rapid and synchronous collapse of marine and terrestrial ecosystems during the end-Permian biotic crisis: Geology, v. 29, p. 351-354.

Viglietti, P.A., Smith, R.M.H., and Compton, J.S., 2013, Origin and palaeoenvironmental

significance of Lystrosaurus bonebeds in the earliest Triassic of the Karoo Basin, South Africa: Palaeogeography, Palaeoclimatology, Palaeoecology, v. 392, p. 9-21.

Visscher, H., Brinkhuis, H., Dilcher, D.L., Elsik, W.C., Eshet, Y., Looy, C.V, Rampino, M.R., and Traverse, A., 1996, The terminal Paleozoic fungal event: Evidence of terrestrial ecosystem destabilization and collapse: Proceedings of the National Academy of Science of the United States of America, v. 93, p. 2155-2158.

Visser, J.N.J., and Loock, J.C., 1978, Water depth in the main Karoo Basin, South Africa, during the Ecca (Permian) sedimentation: Transactions of the Geological Society of South Africa, v. 81, p. 185-191.

Ward, P.D., Montgomery, D.R., and Smith, R.M.H., 2000, Altered river morphology in South Africa related to the Permian-Triassic extinction: Science, v. 289, p. 1740-1743.

Ward, P.D., Botha, J., Buick, R., Dekock, M.O., Erwin, D.H., Garrison, G., Kirschvink, J., and Smith, R.M.H., 2005, Abrupt and gradual extinction among Late Permian land vertebrates in the Karoo Basin, South Africa: Science, v. 307, p. 709-714.

Yin, H.F., Zhang, K.X., Tong, J.N., Yang, Z.Y., and Wu, S.B., 2001, The Global Stratotype Section and Point (GSSP) of The Permian–Triassic boundary: Episodes, v. 24, p. 102–114.

Yin, H., Feng, Q., Lai, X., Baud, A., and Tong, J., 2007, The protracted Permo-Triassic crisis and multi-episode extinction around the Permian-Triassic boundary: Global and Planetary Change, v. 55, p. 1-20.

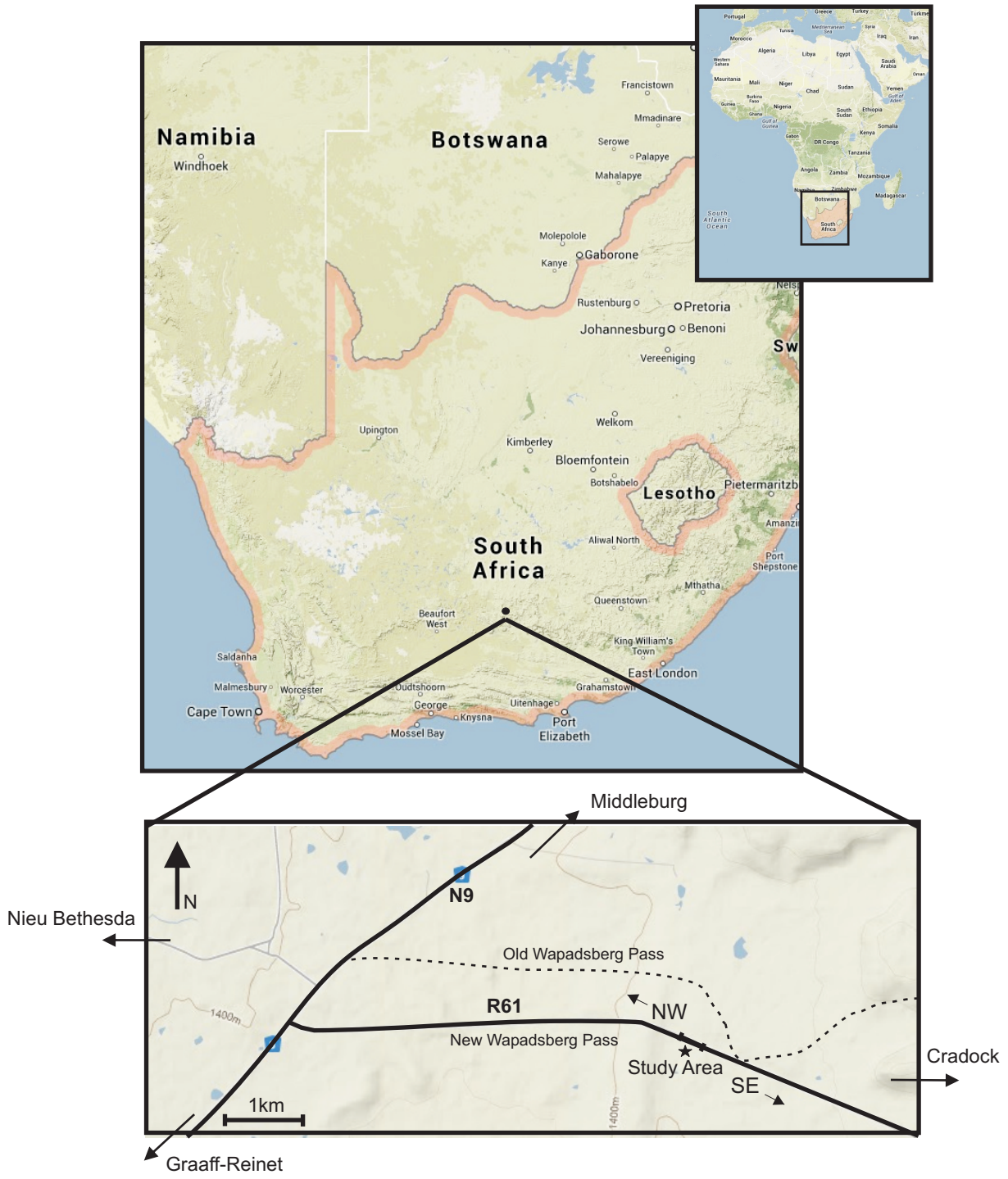

Figure 1. Study Area locality: Roadcut along the R61 Highway, Eastern Cape Province, South Africa.

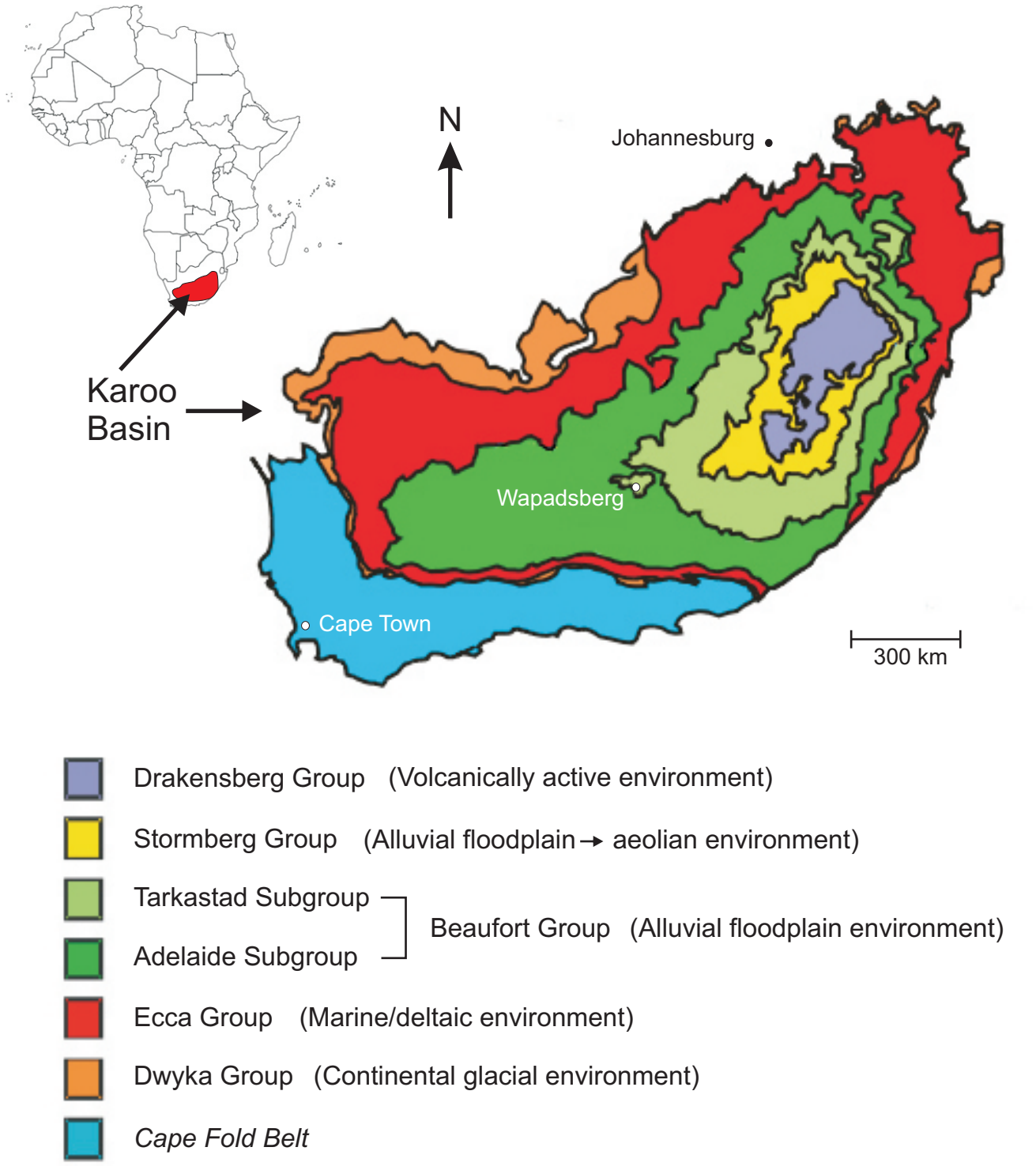

Figure 2. Simplified geologic map of the Karoo Basin showing the major groups of the Karoo Supergroup and the Wapadsberg Pass locality (Modified after Coney (2005)).

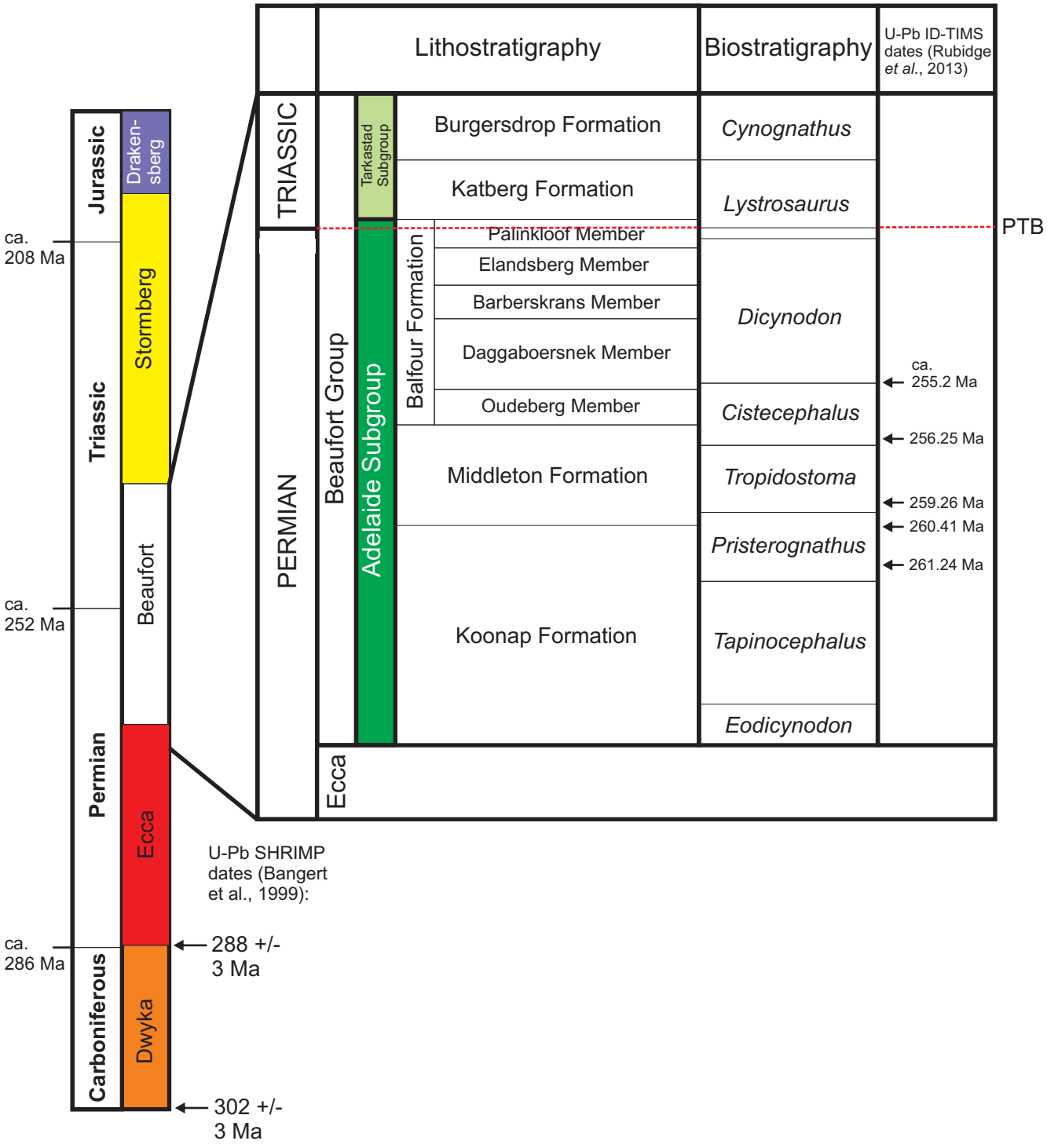

Figure 3. Classification of the Karoo Supergroup based on lithostratigraphy and biostratigraphy (Modified after Rubidge *et al.* (2013)). Included are dates constraining the Dwyka Group and dates from the Lower Beaufort Group.

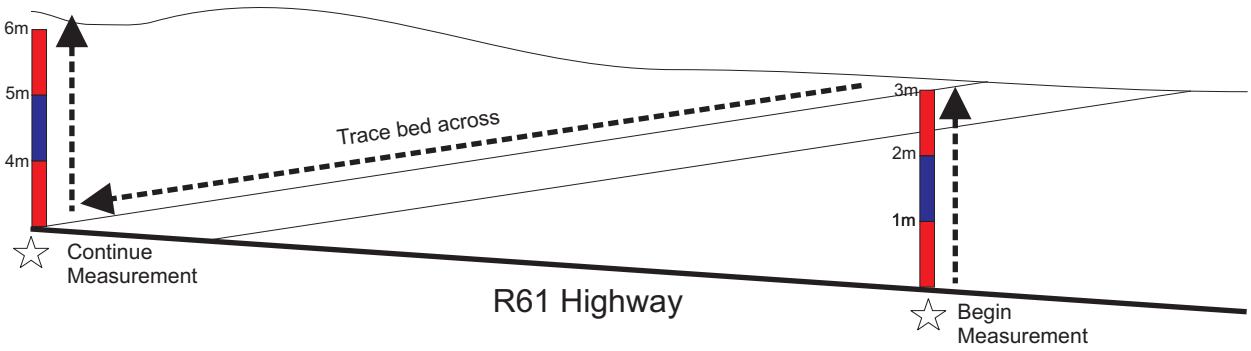

Figure 4. An illustration showing the method used to measure the section. This method was aided by the use of a 1.5m Jacob's staff with leveling sight in order to ensure accuracy.

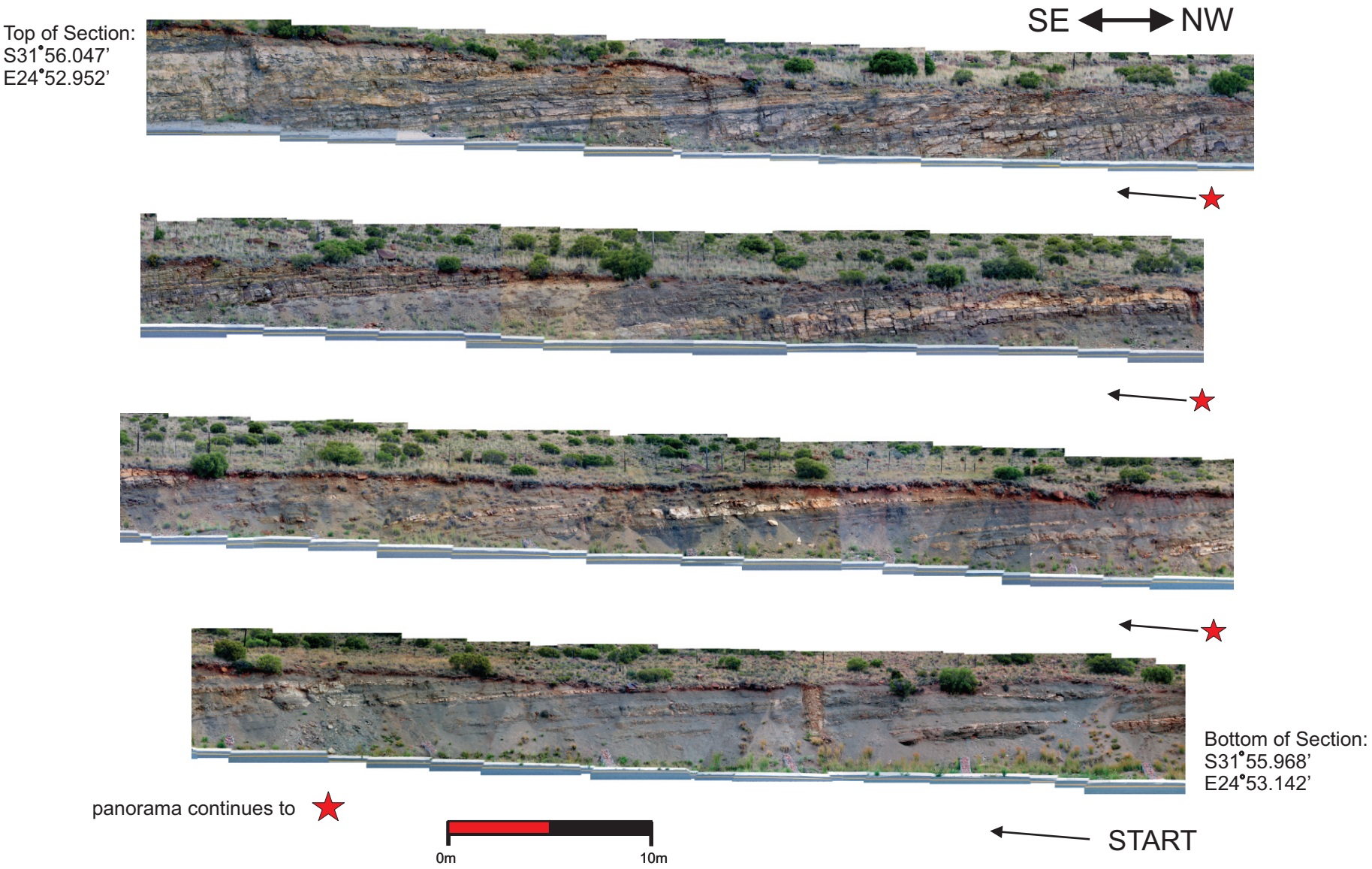

Figure 5. Complied photomosaic showing the extent of the study section along the R61 highway at New Wapadsberg Pass.

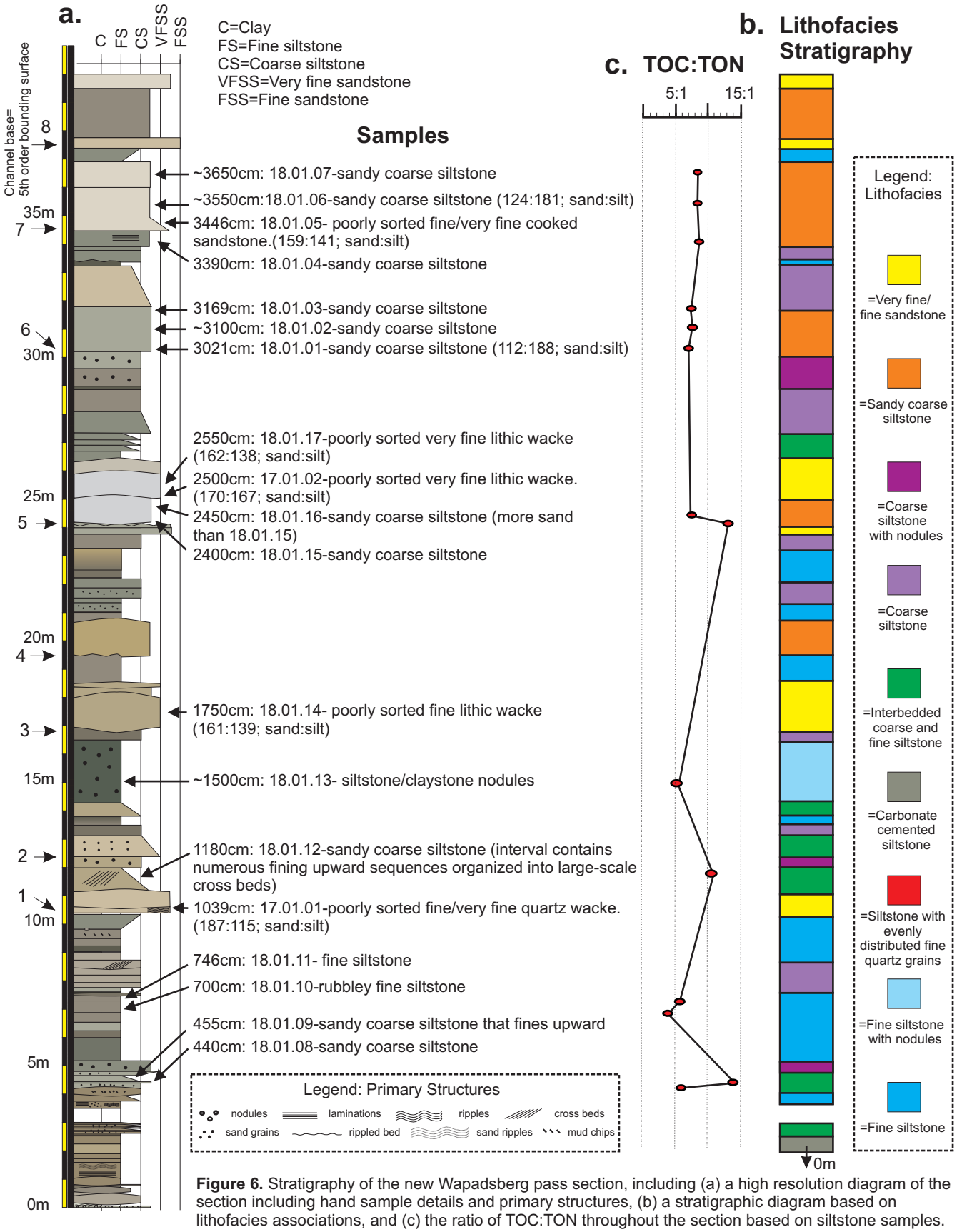

Figure 6. Stratigraphy of the new Wapadsberg pass section, including (a) a high resolution diagram of the section including hand sample details and primary structures, (b) a stratigraphic diagram based on lithofacies associations, and (c) the ratio of TOC:TON throughout the section based on siltstone samples.

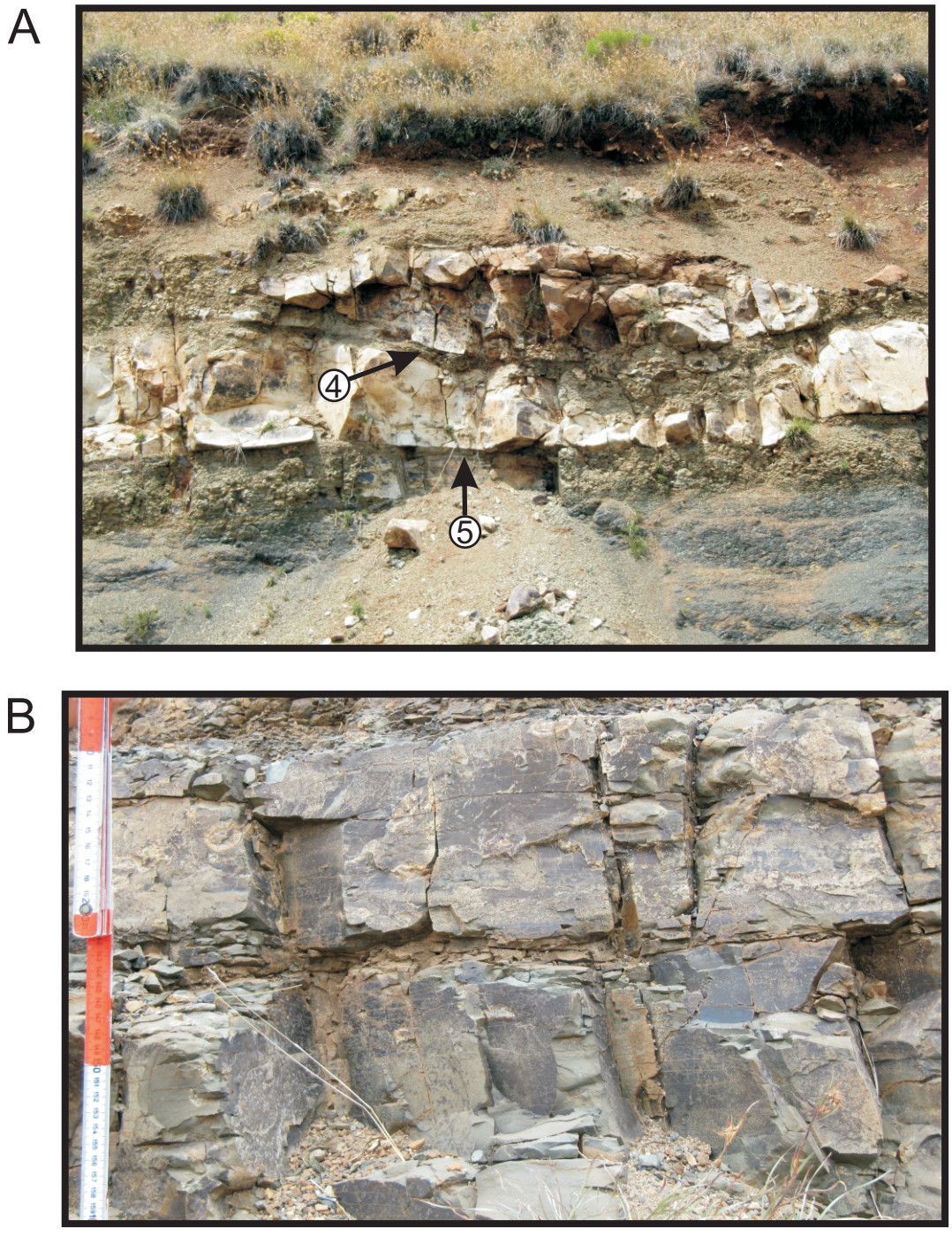

Figure 7. A) A lenticular sandstone underlain by a 5th order bounding surface, following Miall (1996). A 4th order bounding surface marks the bottom of the sandstone lens. B) An example of the sandy coarse siltstone lithofacies.

A

B

Figure 8. A) A series of fining upward sequences where beds transition from sandy coarse siltstone to fine siltstone. This is an example of the alternating fine/coarse siltstone facies. B) An example of the claystone facies.

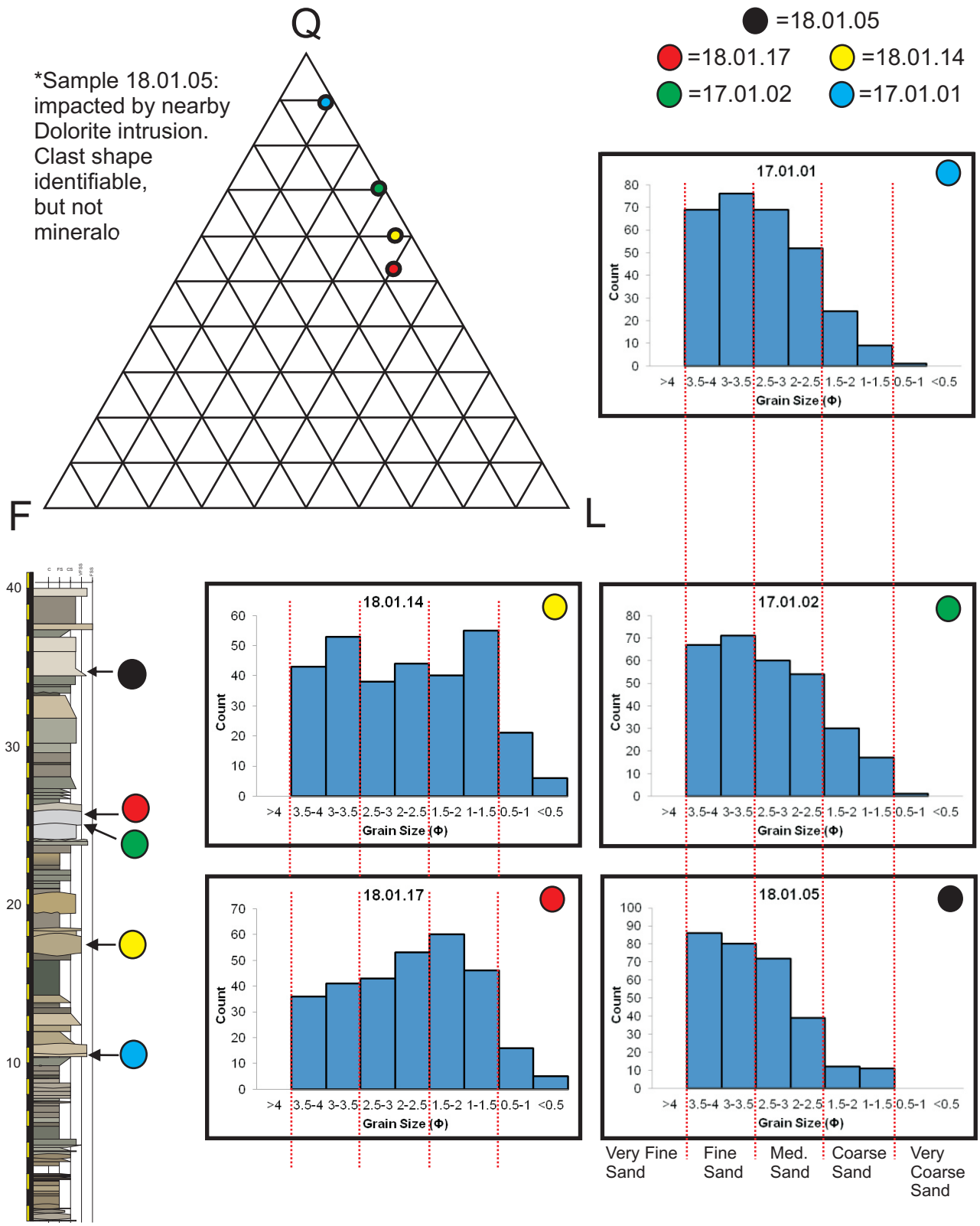

Figure 9. Mineralogy (QFL) and grain size distribution for the 5 sandstone samples collected.

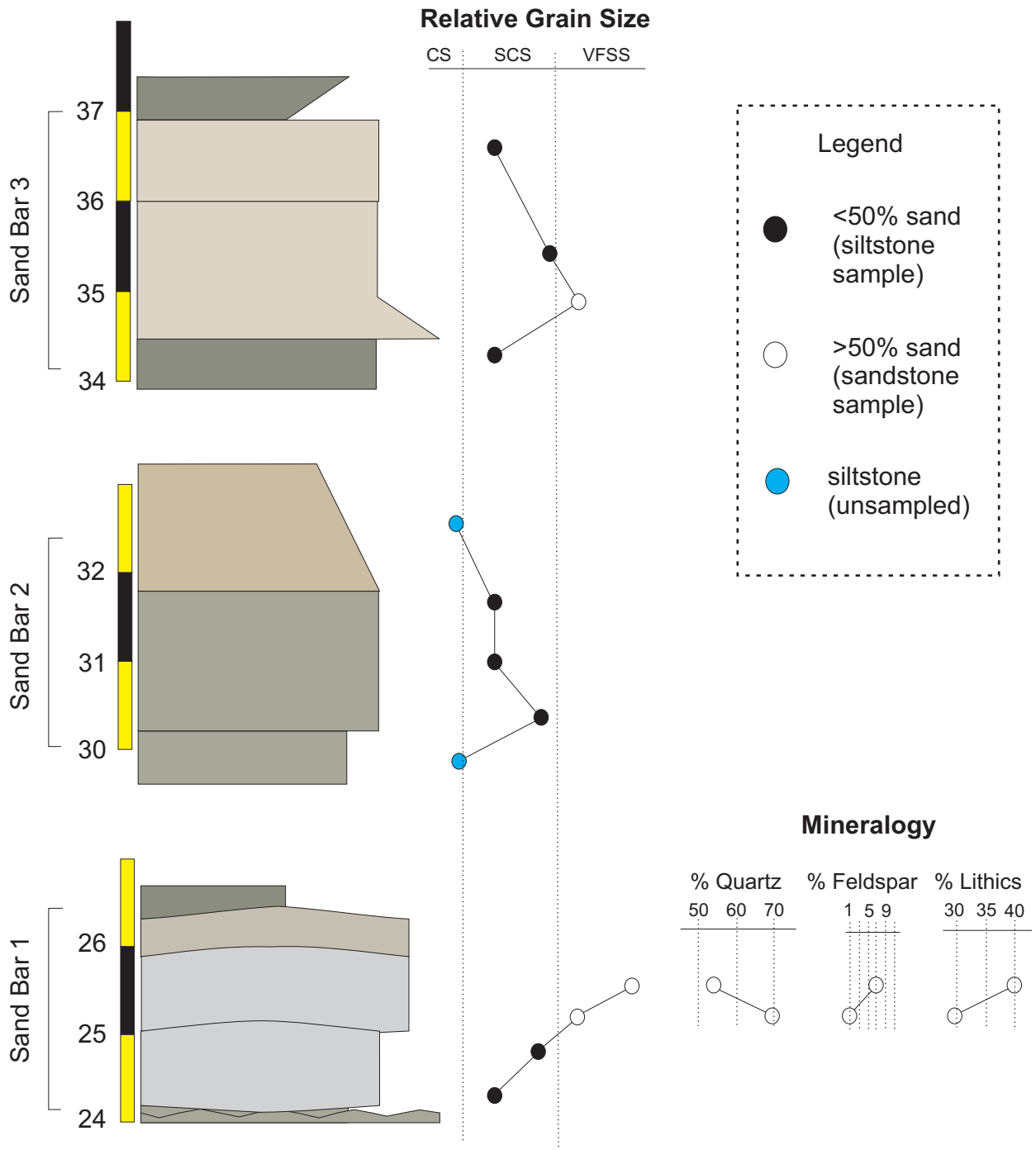

Figure 10. The relative grain size and mineralogical changes of 3 sand bar complexes.

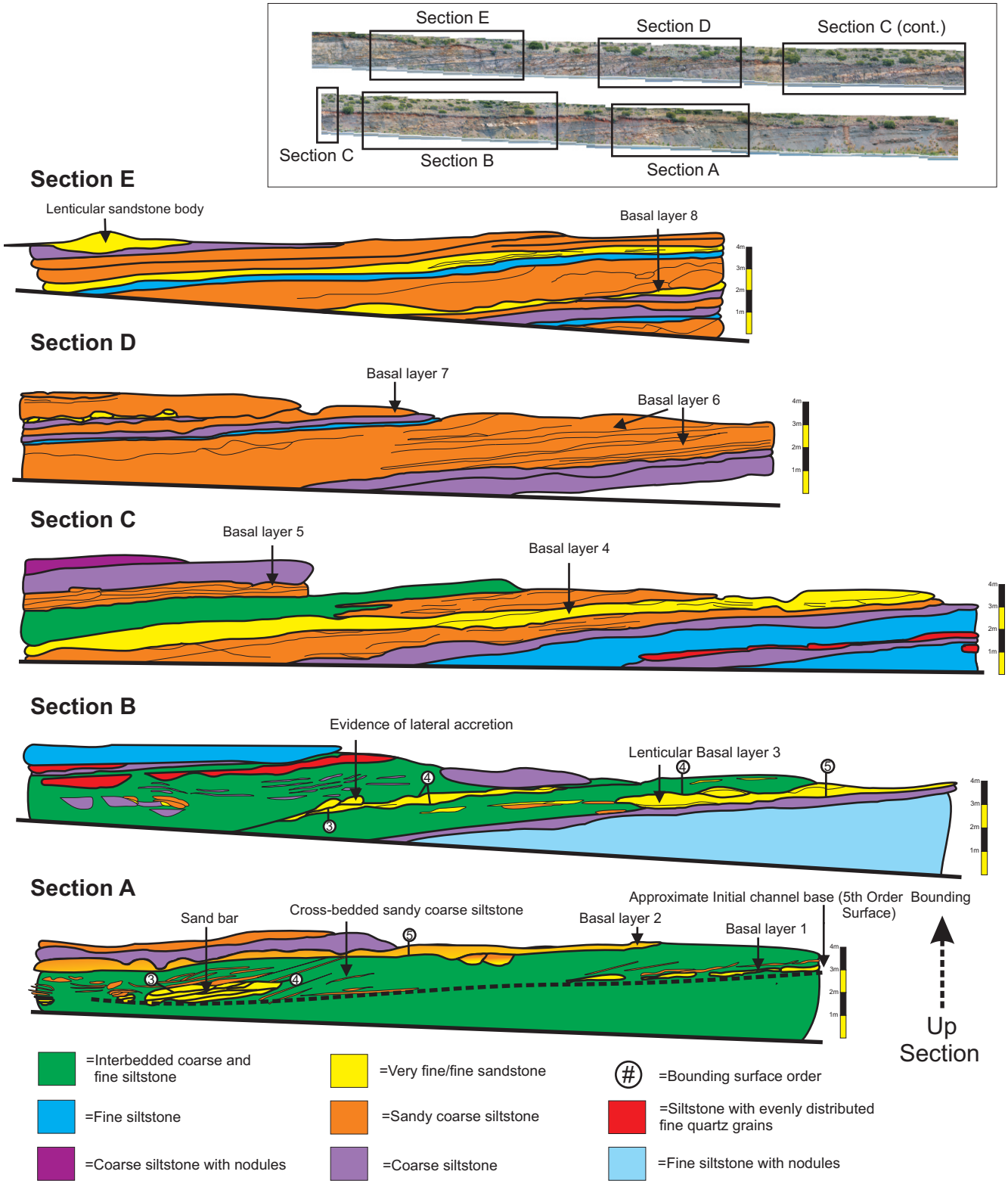

Figure 11. Five representative parts of the stratigraphic section colored by lithofacies. Some bounding surfaces and their classification based on Miall (1996) are also shown.

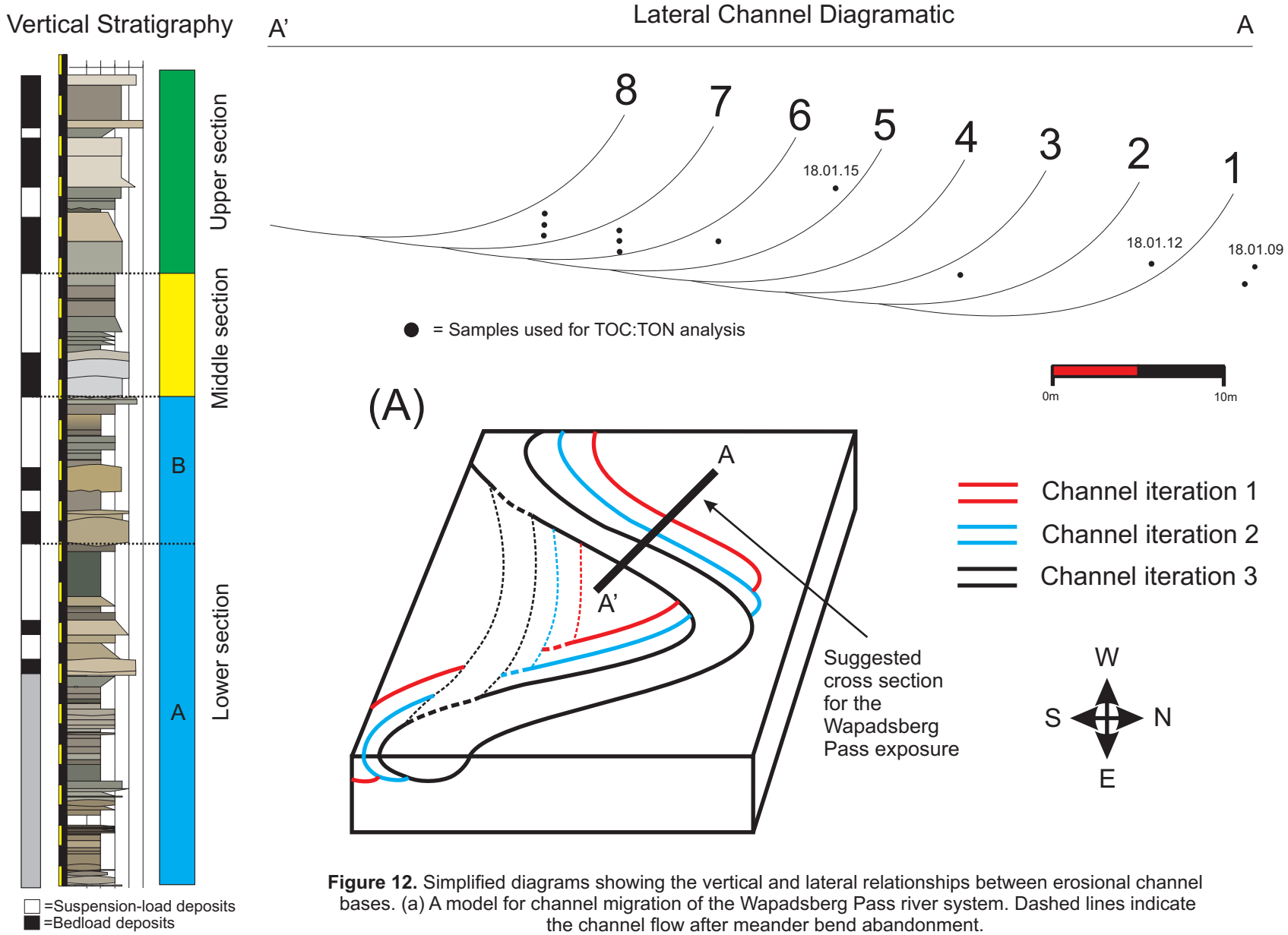

Figure 12. Simplified diagrams showing the vertical and lateral relationships between erosional channel bases. (a) A model for channel migration of the Wapadsberg Pass river system. Dashed lines indicate the channel flow after meander bend abandonment.

Lithofacies	Grain Size	Grain Size Characteristics	Geometry & Bed Thickness	Primary Structures	Contacts	Diagenetic Features	Color	Bedload or Suspension Load Deposit
Very fine-fine wacke sandstone	very fine-fine sand (>50%) with coarse silt	quartz or lithic wacke; moderate-porrly sorted; negatively skewed; mainly platykurtic	planar, lenticular; laterally accreted units; thickness 0.5-3 m	mm-scale ripples	erosional below; sharp or gradational above	none	greenish grey; yellowish grey; light grey	bedload
Sandy coarse siltstone	coarse silt (>50%) with very fine-fine sand	coarse siltstone with sand grains	planar, lenticular; thickness up to 2 m	mm-scale laminations or ripples	erosional, sharp, or gradational below; sharp or gradational above	none	greenish grey-light yellowish grey	primarily bedload; some thin beds within suspension load deposits
Coarse siltstone	coarse silt with minimal fine sand grains	grains size realtively uniform	planar, lenticular; thickness 0.1-0.9 m	none	sharp or gradational above and below	none	olive grey-greenish grey	suspension load
Coarse siltstone with nodules	coarse silt with minimal fine sand grains	grains size realtively uniform	planar; thickness 0.3-0.7 m	none	sharp above and below	2-5 cm nodules occur in horizons	olive grey-greenish grey	suspension load
Alternating fine/coarse siltstone	fine silt; coarse silt	numerous fining-upward sequences	planar units overall; some fine silstone beds are lenticular	units may be organized into large-scale crossbeds	sharp below; sharp or gradational above	none	light olive grey-yellowish grey-greenish grey	suspension load
Carbonate cemented coarse and fine siltstone	fine silt; coarse silt	some fine sand grains incorporated	planar, lenticular; thickness 0.1-0.3 m	none	sharp above and below	carbonate cement	light olive grey-greenish grey	suspension load
Fine siltstone	fine silt	uniform grain size	planar; thickness > 0.1 m	mm-scale laminations; mm-scale ripple; mm-scale mudchips	sharp or gradational above and below	none	light olive grey-dark greenish grey	suspension load
Fine siltstone with nodules	fine silt	uniform grain size	planar; thickness 2 m	none	sharp above and below	2-5 cm nodules occur in 5 horizons	dark greenish grey	suspension load

Fine siltstone with dispersed quartz grains	fine silt; fine sand	fine sand grains distributed throughout fine siltstone	planar; thickness < 0.75 m	none	sharp or gradational above and below	none	light olive grey- dark greenish grey	suspension load
Claystone	clay	uniform grain size	planar; thickness < 5 cm	none	sharp above and below	none	light greenish grey; yellowish grey	suspension load

Table 1. Lithofacies designations and characteristics for the Wapadsberg Pass Section.

Stratigraphic Position	Sample	Carbon	Hydrogen	Nitrogen	TOC (average of 3 runs)	TON (average of 3 runs)	TOC:TON
440cm	180108	0.33	0.1	0.05	0.38	0.06	6.39
	b	0.4	0.11	0.06			
	c	0.42	0.18	0.07			
455cm	180109	0.8	0.27	0.06	0.75	0.05	14.13
	b	0.81	0.14	0.05			
	c	0.65	0.12	0.05			
700cm	180110	0.29	0.38	0.06	0.26	0.06	4.59
	b	0.26	0.3	0.06			
	c	0.23	0.29	0.05			
750cm	180111	0.4	0.33	0.06	0.49	0.08	6.08
	b	0.63	0.29	0.1			
	c	0.43	0.36	0.08			
1180cm	180112	0.62	0.17	0.06	0.70	0.06	11.05
	b	0.54	0.1	0.05			
	c	0.94	0.15	0.08			
~1500cm	180113	0.53	0.72	0.07	0.54	0.09	6.00
	b	0.65	0.52	0.12			
	c	0.44	0.6	0.08			
2400cm	180115	0.69	0.41	0.05	0.61	0.05	13.14
	b	0.65	0.23	0.05			
	c	0.5	0.19	0.04			
2450cm	180116	0.2	0.09	0.02	0.41	0.05	7.63
	b	0.64	0.12	0.09			
	c	0.38	-0.01	0.05			
3021cm	180101	0.51	0.52	0.1	0.73	0.10	7.55
	b	1.02	0.42	0.11			
	c	0.66	0.28	0.08			
~3100cm	180102	0.42	0.24	0.05	0.40	0.05	8.00
	b	0.31	0.19	0.04			
	c	0.47	0.24	0.06			
3169cm	180103	0.34	0.3	0.04	0.32	0.04	7.92
	b	0.31	0.25	0.04			
	c	0.3	0.21	0.04			
3390cm	180104	0.4	0.21	0.05	0.41	0.05	9.00
	b	-	-	-			
	c	0.41	0.1	0.04			
~3550cm	180106	0.57	0.33	0.07	0.49	0.06	8.65
	b	0.36	0.18	0.04			
	c	0.54	0.13	0.06			
~3650cm	180107	0.39	0.28	0.05	0.32	0.04	8.73
	b	0.22	0.17	0.02			
	c	0.35	0.05	0.04			
						Section Average:	8.49

Table 2. A summary of elemental analysis of siltstone samples (C,H, and N) and associated TOC:TON ratios.

Stratigraphic Position	Sample	Lithologic designation	Sand:Silt
1039 cm	17.01.01	fine/very fine sandstone	187:115
1750 cm	18.01.14	fine sandstone	161:139
2450 cm	18.01.16	sandy coarse siltstone	130:170
2500 cm	17.01.02	fine sandstone	170:167
2550 cm	18.01.17	very fine sandstone	162:138
3021 cm	18.01.01	sandy coarse siltstone	112:188
3446 cm	18.01.05	fine/very fine sandstone	159:141
3550 cm	18.01.06	sandy coarse siltstone	124:181

Table 3. Summary of sand:silt ratios for field-identified sandstones.

Sample	**17.01.01 (1039 cm)**	**17.01.02 (2500 cm)**	**18.01.05 (3446 cm)**	**18.01.14 (1750 cm)**	**18.01.17 (2550 cm)**
Mean (Φ)	2.91 Fine sand	2.81 Fine sand	3.01 Very fine sand	2.31 Fine sand	2.27 Fine sand
Median (Φ)	2.96 Fine sand	2.84 Fine sand	3.09 Very fine sand	2.32 Fine sand	2.16 Fine sand
Standard Deviation (Φ)	0.75 Moderately sorted	0.76 Moderately sorted	0.7 Moderately sorted	1.03 Poorly sorted	0.98 Moderately sorted
Skewness (Φ)	-0.17 Coarse skewed	-0.23 Coarse skewed	-0.2 Coarse skewed	-0.05 Nearly symmetrical	0.06 Nearly symmetrical
Kurtosis (Φ)	0.86 Platykurtic	0.82 Platykurtic	1.05 Mesokurtic	0.72 Platykurtic	0.88 Platykurtic

Table 4. Phi values for mean, median, standard deviation, skewness, and kurtosis for grains of the 5 sandstone samples.

Sample	Stratigraphic Position	Quartz (%)	Feldspar (%)	Lithics (%)
17.01.01	1039 cm	268 (89)	5 (2)	27 (9)
17.01.02	2500 cm	211 (70)	3 (1)	86 (29)
18.01.05*	3446 cm	-	-	-
18.01.14	1750 cm	180 (60)	9 (3)	111 (37)
18.01.17	2550 cm	158 (53)	21 (7)	121 (40)

*=mineralogy not identifiable

Table 5. Grain mineralogy (QFL) for sandstone samples.